ABSTRACT

WRIGHT, ANDREW ARMEAN. Mathematical Models of Various Effects on a Normal Menstrual Cycle. (Under the direction of Mette Olufsen.)

Since the rise of our understanding of the hormonal dynamics within the menstrual cycle, there have been investigations into altering the behavior of these dynamics through introduction of exogenous hormones with the aim of achieving a contraceptive state. Since the 19th century these hormonal contraceptives have been studied for efficacy and safety. Large changes have been made throughout that time mostly in adjusting dosages to more safe levels than where they began. An important new tool in studying these interactions is mathematical modeling in an attempt to capture a system's behavior and predict some drug behavior before applying it to biological specimens. In recent history study of menstrual cycle dynamics and the effect of hormonal contraceptives have expanded largely. Most research on contraceptive drugs has taken place since the 19th century. There has been a rise in the need for understanding of the hormonal dynamics and the specific effect of hormonal treatments aimed at contraceptives. The main topic of this dissertation is a discussion of three mechanistic models of the menstrual cycle: a model of follicle waves in cycling women, an analysis of parameters in the cycle possibly associated with a stress reaction, and a model of hormonal contraceptives applied to the system. The first chapter gives an overview of general biology for the menstrual cycle and a brief discussion of how the models are formulated from these dynamics. The second chapter discusses the phenomenon of follicle waves. In this system multiple waves of follicular stimulating hormone (FSH) during the cycle can lead the the selection of more than one dominant follicle. This model also includes a term for atresia a process not considered in the other two formulations. Results of both a two and three follicle wave cycle are discussed. The third chapter concerns the relationship between the hypothalamus-pituitary-ovarian axis (HPO axis) and the hypothalamus-pituitary-adrenal axis (HPA axis). It has been observed that stress can alter the natural balance of the menstrual cycle leading to dysfunctional cycles. Parameters associated with luteinizing hormone (LH) synthesis were suspected as likely places the body's main stress hormone (cortisol) may affect the biology. Dynamical analysis of three parameters associated with the LH synthesis was performed and discussed. The fourth chapter in the dissertation provides an example of the effects of hormonal contraceptives in the model. Relative data for a progesterone based contraceptive and a combined estrogen-progesterone contraceptive was used to tune the model though it was used for overall behavior and not for specific optimization. Additional components in the model in the form of two autocrine effects were added to account for dynamics important in the administration of hormonal contraceptives. Important considerations in this model included model behavior when contraceptives were applied, the efficiency of a combined low dose, as well as a return to a normal health cycle once the dosing was removed.

Mathematical Models of Various Effects on a Normal Menstrual Cycle

by
Andrew Armean Wright

A dissertation submitted to the Graduate Faculty of
North Carolina State University
in partial fulfillment of the
requirements for the Degree of
Doctor of Philosophy

Biomathematics

Raleigh, North Carolina

2022

APPROVED BY:

James Selgrade	Alun Lloyd
Alen Alexanderian	Mette Olufsen Chair of Advisory Committee

DEDICATION

I would like to dedicate my efforts here to my parents. They have supported and encouraged me through this whole process. I would not have made it here without them. I would also like to thank Mette Olufsen and Alun Lloyd who worked with me through a great many issues and always provided the help that I needed. I owe my experience and education to their understanding and help throughout my academic career.

BIOGRAPHY

I began my academic career in 2008 at NC State. I entered in biochemistry and changed to pure mathematics after the first year. In the end of my undergraduate experience I met Dr. Mette Olufsen who I began working with on cardiovascular dynamics. I remained at NC State for graduate school pursuing my PhD in biomathematics and continuing my work with Dr. Olufsen. We published a paper relating to cardiovascular dynamics of the head up tilt. After taking a class with Dr. James Selgrade in dynamical analysis, I went on to work with him on various formulations of the mechanistic menstrual cycle model. A paper was published on the phenomenon of follicle waves which I contributed to in the form of numerical dynamical analysis of the system. I later worked at Merck Pharmaceuticals adapting a form of Dr. Selgrade's model to be used in conjunction with hormonal contraceptives. The project went on to publish the work and was my first primary authorship on a paper. I have begun work at Applied Biomath in the field of pharmakokenetics and pharmacodynamics.

TABLE OF CONTENTS

LIST OF TABLES

LIST OF FIGURES

CHAPTER

1

INTRODUCTION

The menstrual cycle is the periodic cycle existing in mammalian females. The human cycle is approximately 28 days. This process is the result of a complex interaction between ovarian hormones and pituitary hormones that have a distictive cycle. A significant body of research examines how to disrupt or extend this cycle leading to a contraceptive state. An emerging method of studying these interactions is to model them mathematically. This dissertation expands and examines the body of work devised by Selgrade *et al.* [Sel99; Sel09; Sel10]. We discuss these topics in five chapters. The main focus of these studies are follicle waves a unique phenomenon of the menstrual cycle (chapter 3), the impact of stress on the system (chapter 4), and the effects of hormonal contraceptives (chapter 5). A description of general model composition throughtout the dissertation is also shown. The last chapter contains a discussion of the three papers and their results.

Chapter 2: Menstrual Cyle
This chapter discusses the associated biology of the menstrual cycle including the relevant hormones from the ovaries, hypothalamus, and pituitary. General biological mechanisms and relationships are discussed. The formulation of the mechanistic model of the mestrual cycle is explained. A lumped model of the hypothalamus and pituitary is presented combined with a model of the ovarian cycles and resulting hormone production are combined to the full model [Sel99].

Chapter 3: Follicle Waves

The second chapter includes the paper by *Panza NM, Wright AA, Selgrade JF (2016). Delay differential equation model of follicle waves in women. J Biol Dyn 10(1):200–221.* This study discusses modeling follicle waves, a phenomenon that can lead to multiple primary follicles being selected. My role consisted of adapting the model for use with DDEBifTool a MATLAB package for use in dynamical analysis of delay differential equations. I contributed to the parameter analysis including sensitivity analysis and dynamical analysis [Pan16].

Chapter 4: Stress

The third chapter aims to investigate the effects of stress on the menstrual cycle model. This was accomplished by dynamical analysis of parameters in the Selgrade model that may be associated with stress effects that can lead to dysfunctional cycles. The hyopthalamus-pituitary-adrenal (HPA) axis interaction with the hypothalamus-pituitary-ovarian (HPO) axis can cause dysfunctional cycles. Various parameters associated with the synthesis of luteinizing hormone (LH) were analyzed using DDEBifTool for dynamical behavior. Of concern mainly is reduction in LH surge to non ovulatory levels and existence of two stable cycles in some situations, one ovulatory and one anovulatory.

Chapter 5: Contraception

This chapter provides a brief discussion of the history and development of contraceptives is given before the presentation of the model. The rest of the section is taken from the paper *Wright AA, Fayad, GN, Selgrade JF, Olufsen MS (2020). Mechanistic model of hormonal contraception. PLoS Comp Biol. 16(6):e1007848*. My role in this paper consisted of: model modification from original model in [Mar11], optimization and sensitivity analysis of new model, dynamical analysis of dose response using DDEBifTool, and primary contribution to writing of the paper. The focus of the paper was to apply a hormonal based contraceptive to an existing mechanistic menstrual cycle model. A progestin based, and estrogen based, and a combined treatment of hormonal contraceptives were considered, and the progestin and combined were compared with data.

CHAPTER

2

MENSTRUAL CYCLE

2.1 Hormonal Interactions in the Menstrual Cycle

The menstrual cycle refers to the period between menstruations mammals depicted characteristically in Fig 2.1. This section based on material from [Fri11] is dedicated as describing the complex hormonal interaction generating the cycling dynamics. A representation of the menstrual cycle phases is shown in Fig 2.1 including associated hormones with direction from site of production to site of action. The menstrual cycle arises from a complex interaction between the hypothalamus and pituitary in the brain, and the ovaries.

The brain. In the brain a system of capillaries forms a small portal system that flows from the hypothalamus to the anterior pituitary directly below. The portal circulation gives the hypothalamus means to communicate with the pituitary as there is no direct nervous connection. The hypothalamus secretes gonadotropin releasing hormone (GnRH) into this portal system in accordance with stimulation from ovarian hormones as well as feedback from pituitary gonadotropins. Because the half life of GnRH is very small (2-4 minutes), it is only in the portal system that effective levels are found. This means that GnRH must be constantly released, and is done so in a pulsatile fashion with changes in both magnitude and frequency in response to feedback from ovarian hormones and pituitary gonadotropins. These pulsatile secretions are relatively fast taking place every 1-3 hours depending on menstrual cycle phase, and a wide variability exists amongst individuals. The

pulsatile stimulation from GnRH influences the anterior pituitary in both synthesis and release of gonadotropins which results in pulsatile release of pituitary gonadotropins (including luteinizing hormone (LH) and follicular stimulating hormone (FSH)) which influence the ovaries.

The ovaries. The menstrual cycle is made of of two phases: the follicular phase and the luteal phase. In the weeks after a woman is born her ovaries produce a large mass of germ cells (6-7 million). These are the full amount the ovaries will ever contain, and will decrease as they are transformed by mitosis and a meiotic division into an oocyte. Pre-granulosa cells envelope an oocyte and the resulting unit is called a primordial follicle. This process will eventually happen to all oocytes. As the follicle grows and the surrounding granulosa cell layer proliferates, it becomes a primary follicle. From primary follicle stage it is believed that about 85 days pass before ovulation; most of this time is spent without the influence of pituitary gonadotropins. The follicular phase begins when multiple follicles are "recruited" and begin expressing FSH receptors which when stimulated support the follicle's growth. Further growth gives rise to LH receptor expression, and follicles produce ovarian hormones (including progesterone (P4), estradiol (E2), and inhibin A (InhA)) dependent on stimulation by FSH and LH, and follicle maturity. The follicles compete for FSH (and later LH) and a single follicle if sufficiently stimulated by gonadotropins will advance to ovulation. Follicles may become arrested at any point during this process through a process of atresia consisting of a break down in granulosa activity eventually ending in apoptosis. All follicles that were "recruited" and unable to reach ovulation (all but one in a normal situation) will go through this process. During ovulation the follicle ruptures and releases the oocyte through complex and not well understood mechanisms. The granulosa cells on the ruptured follicle are luteinized and the structure becomes the corpus luteum. This marks the beginning of the luteal phase. During the luteal phase the oocyte (now called an ovum) is ready for fertilization and the corpus luteum produces P4 and E2 with support from low levels of LH. After about 14 days if fertilization has not taken place, menstruation occurs and the cycle begins again.

In the beginning of the follicular phase, follicles produce small amounts of E2 inhibiting LH release. As a follicle develops into a dominant follicle, it begins producing E2 in much larger quantities, and at a critical point of E2 concentration in the blood, the inhibitory effect E2 has on LH release becomes overwhelmed by a rapid increase in LH synthesis also due to E2. This massive change in synthesis is called the LH surge and is necessary for ovulation to occur marking the end of the follicular phase. Near the end of the follicular phase InhA is secreted by the follicles which reduces production of FSH and aids entering the luteal phase. After ovulation the corpus luteum begins producing large amounts of P4 and InhA. In the late luteal phase production of InhA decreases allowing for increase production in FSH and production of E2 begins, both priming the cycle for the next follicular phase.

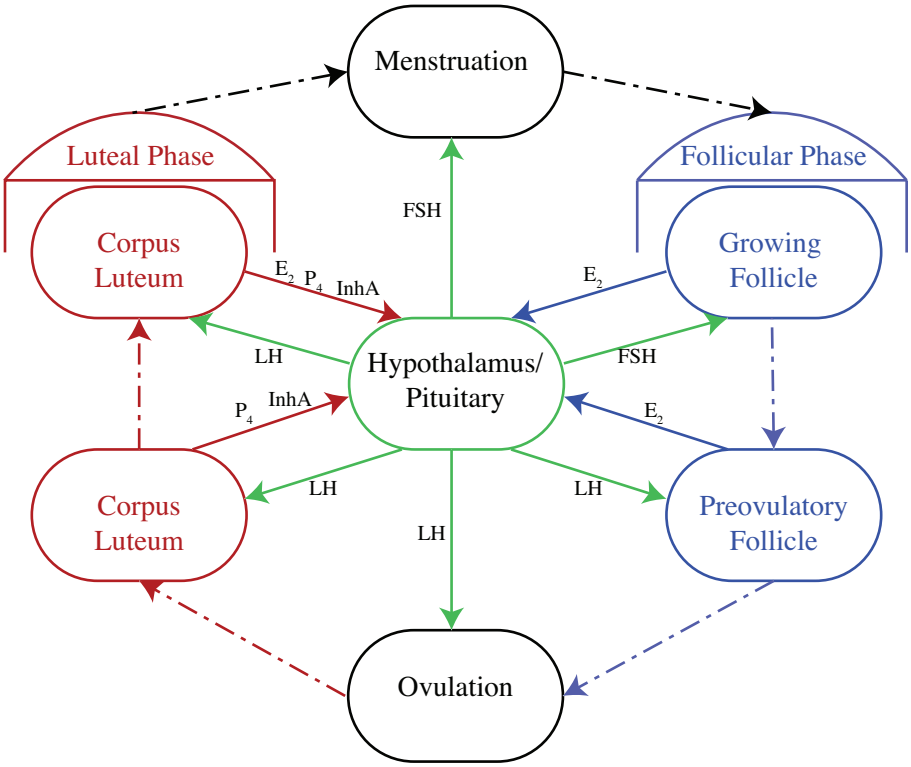

Figure 2.1 Menstrual cycle phases. Phases of the menstrual cycle and associated hormones in effect for each stage. Solid lines indicate an effect from hormones. Dotted lined indicate movement through the menstrual cycle phases. Blue colored chambers and lines indicate an associateion with the follicular phases, and red lines indicate an association with the luteal phase. The green chambers and lines indicates pituitary hormone storage and release during the phases.

2.2 Formulation of Menstrual Cycle Model

Several mathematical studies have examined the dynamics of the menstrual cycle varying in the number of details included to descibe the hormonal interactions [Bog72a; Bog72b; LP92; HC03; Rei07; Sel99; Rob13; Che14]. A more detailed review of menstrual cycle modeling literature is included in the following chapters describing specific instances of this model. One of the more prominent contributions include work done by Selgrade *et al.*[Sel99; Sel09; Sel10]. The work presented in this dissertation uses model formulations taken originally from [Sel99]. The formulation of the Selgrade models begins with two seperate models: one of the hypothalamus and pituitary and one of the ovaries. The two basic sub-models depicted in Fig 2.2 form the menstrual cycle model. The first is a lumped model of the hypothalamus and the pituitary which predicts synthesis and release of gonadotropins based on circulating concentrations of ovarian hormones (E2, InhA, P4). The second models the ovaries, accounting for ovarian phases in conjunction with auxiliary equations predicting ovarian hormone production. In Fig 2.2 the ovarian phase model shows the two phases of the menstrual cycle into multiple stages representing amount of active tissue in that stage. This distribution is used to predict production of ovarian hormones in the auxiliary equations.

2.2.0.1 Hypothalamus and pituitary model

The lumped model (Eqs (2.1)-(2.4)) of the hypothalamus and pituitary predicts synthesis and release of FSH and LH as a function of serum concentrations of E2, P4, and InhA. Dynamics of each pituitary hormone consists of two equations (Eqs (2.1)-(2.2) for LH and Eqs (2.3)-(2.4) for FSH). The reserve pool of hormone H (either FSH of LH) designated RP_H tracks the mass of stored gonadotropin H within the pituitary. This is where synthesis occurs and hormones are stored before release. Once released, the mass is scaled by blood volume v. The reserve pool is described by two factors, a positive synthesis term and a negative release term. The hormone concentration H consists of a positive term, denoting the release term from the reserve pool scaled by blood volume, and a negative linear term representing clearance of the hormone from the blood. Also present in the synthesis term for FSH is a delay for Inh. The biological process for inhibin's effect is lengthy and we account for this by blood levels taking over a day to have an effect [Fra89].

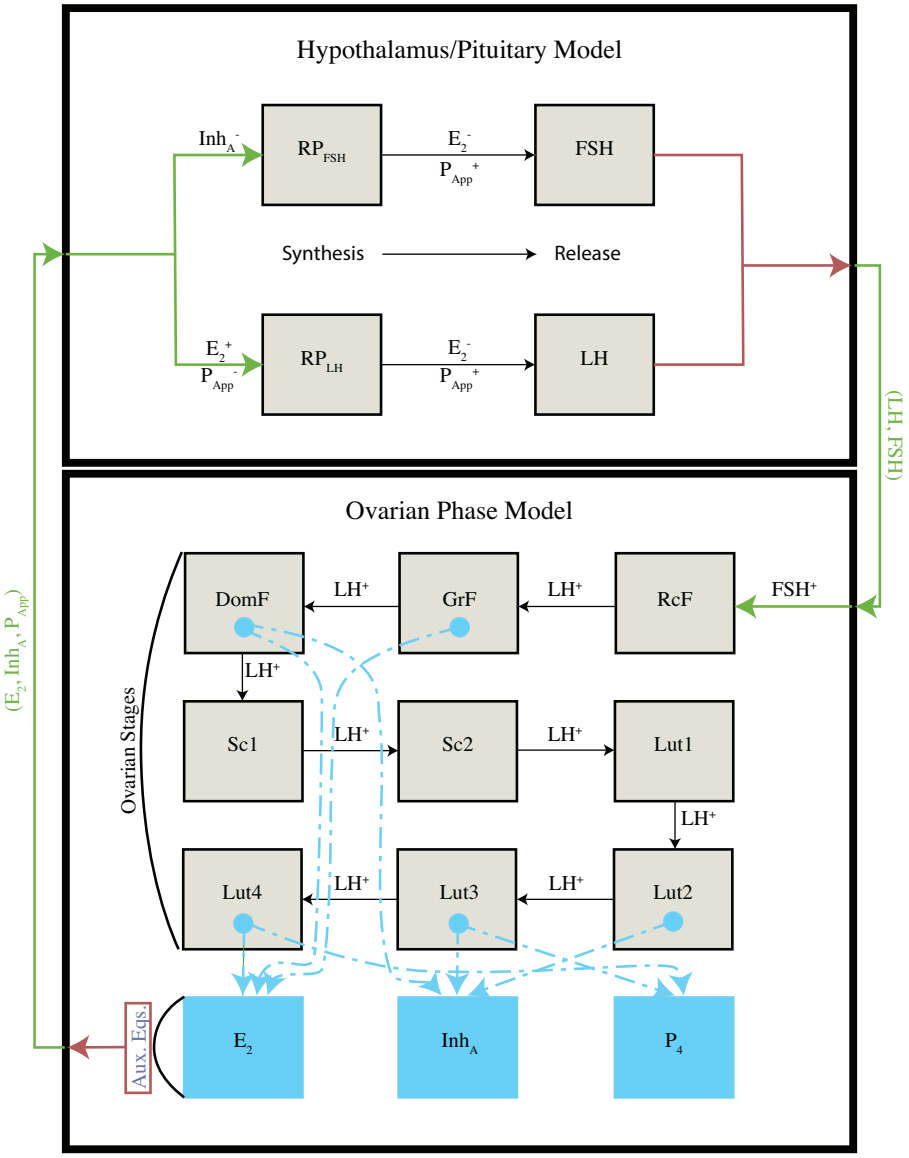

Figure 2.2 Full model diagram. The model diagram shows all the states broken into the two sub-models. Black arrows represent movement between stages within a sub-model. The red arrows represent output from a sub-model, and green arrows represent input into a sub-model. A hormone H written as H^+ or H^- has a stimulating or inhibiting effect respectively on movement between chambers or effectiveness of a hormone within the chamber. The blue dotted lines within the ovarian phase model show stages contributing to ovarian hormone production in the auxiliary equations. The grey dotted lines in the ovarian phase model represent autocrine influence of ovarian hormones within the model.

$$\frac{d}{dt}RP_{LH} = \text{synth}_{LH}(E_2, P_4) - \text{rel}_{LH}(E_2, P_4, RP_{LH}) \tag{2.1}$$

$$\frac{d}{dt}LH = \frac{1}{v}\text{rel}_{LH}(E_2, P_4, RP_{LH}) - \text{clear}_{LH}(LH) \tag{2.2}$$

$$\frac{d}{dt}RP_{FSH} = \text{synth}_{FSH}(Inh(t-\tau)) - \text{rel}_{FSH}(E_2, P_4, RP_{FSH}) \tag{2.3}$$

$$\frac{d}{dt}FSH = \frac{1}{v}\text{rel}_{FSH}(E_2, P_4, RP_{FSH}) - \text{clear}_{FSH}(FSH) \tag{2.4}$$

$$\tag{2.5}$$

During a normal cycle estrogen exhibits a 2-stage effect on LH synthesis. Low levels of estrogen will inhibit LH release, but high levels strongly stimulate production. This 2-stage behavior is represented in Eq (2.1): the synthesis term contains a Hill function dependent on E2 which at a critical level of E2 will increase LH synthesis, and in the release term E2 inhibits LH release. The Hill function is the main biological mechanism of the hypothalamus/pituitary model as it is responsible for the mid-cycle LH surge in response to rising E2 levels.

In Eqs (2.1)-(2.4) there are important relationships between E2 and P4 in the synthesis and release of gonadotropins. Although E2 is responsible for simulating synthesis through the Hill function, it also inhibits the release of both LH and FSH which is a secondary mechanism of estrogen based contraception. In this sub-model we also include the secondary contraceptive effect of progestin which inhibits the synthesis of LH. Each model presented in this dissertation uses a various form of these synthesis equations.

2.2.0.2 Ovarian model

The ovarian model tracks sensitive follicle mass as it moves through the biological phases of the menstrual cycle: follicular phase and luteal phase (see Fig 2.1). To simulate a delayed effect the model breaks each of the phases into multiple stages and adds two compartments as a transition from the follicular to luteal phase labeled Sc1 and Sc2 which represent the scarring of the follicle during ovulation. Ovarian hormone production is calculated as a result of the amount of mass in each stage in the auxiliary equations. It is assumed that serum concentrations of the ovarian hormones are at a quasi-steady state, i.e. the hormone concentration is proportional to the masses. This is an assumption formulated in [Bog72a] and used in model construction in the original menstrual cycle model from [Sel99].

A set of structure example equations for the ovarian stages is listed in Eqs (2.6a)-(2.6i) and associated auxiliary equations can see seen in Eqs (2.6j)-(2.6m). The follicular phase is broken into 3 stages: recruited follicle (RcF), growing follicle (GrF), and dominant follicle ($DomF$). The mass tracked cannot be thought of directly as mass of the follicles, but as mass of follicle contributing to

corresponding hormone production. For instance, estrogen is produced by follicles in the mid to late follicular phase and in the late luteal phase, so the auxiliary equation for estrogen (Eq (2.6j)) is proportional to mass in the GrF, $DomF$, and Lut_4. Ovulation is broken into two stages ($Sc1$ and $Sc2$) and the luteal phase into four stages ($Lut1$ through Lut). Equations calculating ovarian hormones ($E2$, $P4$, and Inhibin A (Inh)) assumed proportional to masses in different stages are shown in Eqs (2.6j)-(2.6m). Also in Eq (2.6j) and Eq (2.6k) are where an exogenous doses of estrogen (e_{dose}) and progestin (p_{dose}) respectively are added. It is assumed that the added hormone (progestin or estrogen) acts as the endogenous hormone would. Also described in Eq (2.6l) is a term representing the applied progesterone (P_{app}) to the system. The applied progesterone is meant to encompass dynamics involving progesterone receptor expression due to estrogen. It is in the model everywhere progesterone has an effect. This will be discussed in more detail in the contraceptive components section.

The model equations listed in equations (2.6) contain various parameters we do not discuss in detail here. Later chapters discuss the parameters explicitly that are used in the submodel.

State Variables

$$\frac{d}{dt}RcF = \frac{bFSH + c_1FSH}{(1+P_{app}/Ki_{RcF,P})^{\xi}}RcF - c_2LH^{\alpha}RcF \tag{2.6a}$$

$$\frac{d}{dt}GrF = c_2LH^{\alpha}RcF - c_3LH \cdot GrF \tag{2.6b}$$

$$\frac{d}{dt}DomF = c_3LH \cdot GrF - c_4LH^{\gamma}DomF \tag{2.6c}$$

$$\frac{d}{dt}Sc_1 = c_4LH^{\gamma}DomF - d_1Sc_1 \tag{2.6d}$$

$$\frac{d}{dt}Sc_2 = d_1Sc_1 - d_2Sc_2 \tag{2.6e}$$

$$\frac{d}{dt}Lut_1 = d_2Sc_2 - k_1Lut_1 \tag{2.6f}$$

$$\frac{d}{dt}Lut_2 = k_1Lut_1 - k_2Lut_2 \tag{2.6g}$$

$$\frac{d}{dt}Lut_3 = k_2Lut_2 - k_3Lut_3 \tag{2.6h}$$

$$\frac{d}{dt}Lut_4 = k_3Lut_3 - k_4Lut_4 \tag{2.6i}$$

Auxiliary Equations

$$E_2 = e_0 + e_1GrF + e_2DomF + e_3Lut_4 + e_{dose} \tag{2.6j}$$

$$P_4 = p_0 + p_1Lut_3 + p_2Lut_4 + p_{dose} \tag{2.6k}$$

$$P_{app} = P_4\left(.5 + .5\frac{E_2^{\mu}}{Km_{P_{eff}}^{\mu} + E_2^{\mu}}\right) \tag{2.6l}$$

$$Inh = h_0 + h_1DomF + h_2Lut_2 + h_3Lut_3 \tag{2.6m}$$

CHAPTER

3

FOLLICLE WAVES

3.1 Introduction

This chapter includes the manuscript *Panza NM, Wright AA, Selgrade JF (2016). Delay differential equation model of follicle waves in women. J Biol Dyn 10(1):200–221.* My role in this paper consisted of adapting the model for use with DDEBifTool, sensitivity analysis, and dynamical analysis. The following material is taken verbatim from this paper.

Deterministic, mathematical models consisting of systems of differential equations have been used to describe hormonal regulation of the human menstrual cycle, e.g., Bogumil *et al.*, 1972a, 1972b [Bae03b; Bae03a], Plouffe and Luxenberg, 1992 [LP92], Harris-Clark *et al.*, 2003 [HC03], Reinecke and Deuflhard, 2007 [Rei07], Pasteur and Selgrade, 2011 [Pas11], Roblitz *et al.*, 2013 [Rob13], and Chen and Ward, 2014 [Che14]. This physiological system may be considered dual control because hormones secreted by the hypothalamus and the pituitary glands affect the ovaries and the ovarian hormones affect the brain, see Figure 3.1. Gonadotropin releasing hormone (GnRH) produced by the hypothalamus promotes the synthesis in the pituitary of follicle stimulating hormone (FSH) and luteinizing hormone (LH), which control ovarian activity and ovulation, see [Hot94; Yen05; Zel94]. In turn, the ovaries produce estradiol (E2), progesterone (P4), inhibin A (InhA) and inhibin B (InhB) which influence the synthesis and release of FSH and LH, see [Kar73; Liu83; Wan76].

The menstrual cycle consists of the follicular phase, ovulation and the luteal phase (Figure 3.1) with average duration of 28 days [Tre67]. During the follicular phase, FSH initiates the development

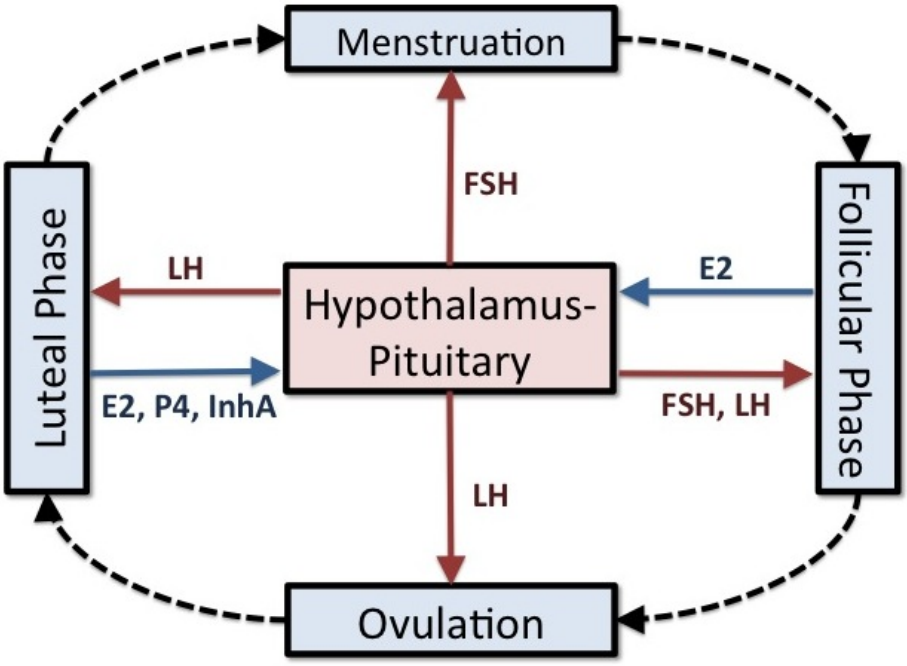

Figure 3.1 The menstrual cycle is controlled by hormones secreted by the hypothalamus and the pituitary and by the ovaries. The cycle begins with menstruation and then follicles develop during the follicular phase. Ovulation occurs followed by the luteal phase during which hormones are secreted for pregnancy. The solid arrows indicate the effects of the gonadotropin hormones (red arrows) on the ovaries and the effects of the ovarian hormones (blue arrows) on the brain during the phases of the cycle.

of 6 to 12 follicles and a dominant follicle is selected to grow to maturity [Ode79; Oje92]. These follicles produce E2 which primes the pituitary to secrete LH in large amounts. At mid-cycle, a rise and fall of LH over a period of 5 days causes the dominant follicle to release its *ovum* and this LH surge is necessary for ovulation. The dominant follicle becomes the corpus luteum, which produces E2 and P4 in preparation for pregnancy. If fertilization does not occur, the corpus luteum atrophies which signals the end of one cycle and the beginning of the next.

In mammals such as cows, horses and sheep, it has been known (Fortune [For94]) that multiple follicles of ovulatory size develop during a single reproductive cycle but only one releases an *ovum*. Because these follicles grow sequentially (e.g., Figure 3.2, Panel a), they are described as follicle waves (Ginther *et al.* [Gin05]). The growth of two or three follicle waves of this sort is stimulated by separate waves of FSH. Because luteal P4 suppresses a LH surge, the ovulatory follicle arises from the cohort that matures after the corpus luteum has atrophied and P4 has diminished. Baerwald *et al.* [Bae03a; Bae03b] have observed follicle waves in normally cycling women. In Baerwald *et al.* [Bae12], two or three follicle waves were illustrated during one menstrual cycle. These waves are initiated by rises in FSH levels. Specifically, for a two wave cycle, the first wave is produced by the early follicular phase rise in FSH and the second wave, by the sharp FSH spike concurrent with the LH surge at mid-cycle (see Figure 3.2, Panel b). The follicle wave corresponding to the mid-cycle FSH spike develops during the luteal phase of the cycle but does not ovulate because of the absence of a luteal LH surge (suppressed by luteal P4) and possibly because the follicle does not reach ovulatory size. When the third wave appears, it develops in response to an unusual late luteal/early follicular rise in FSH (see Figure 3.3, Panel e) as reported by Baerwald *et al.* [Bae12].

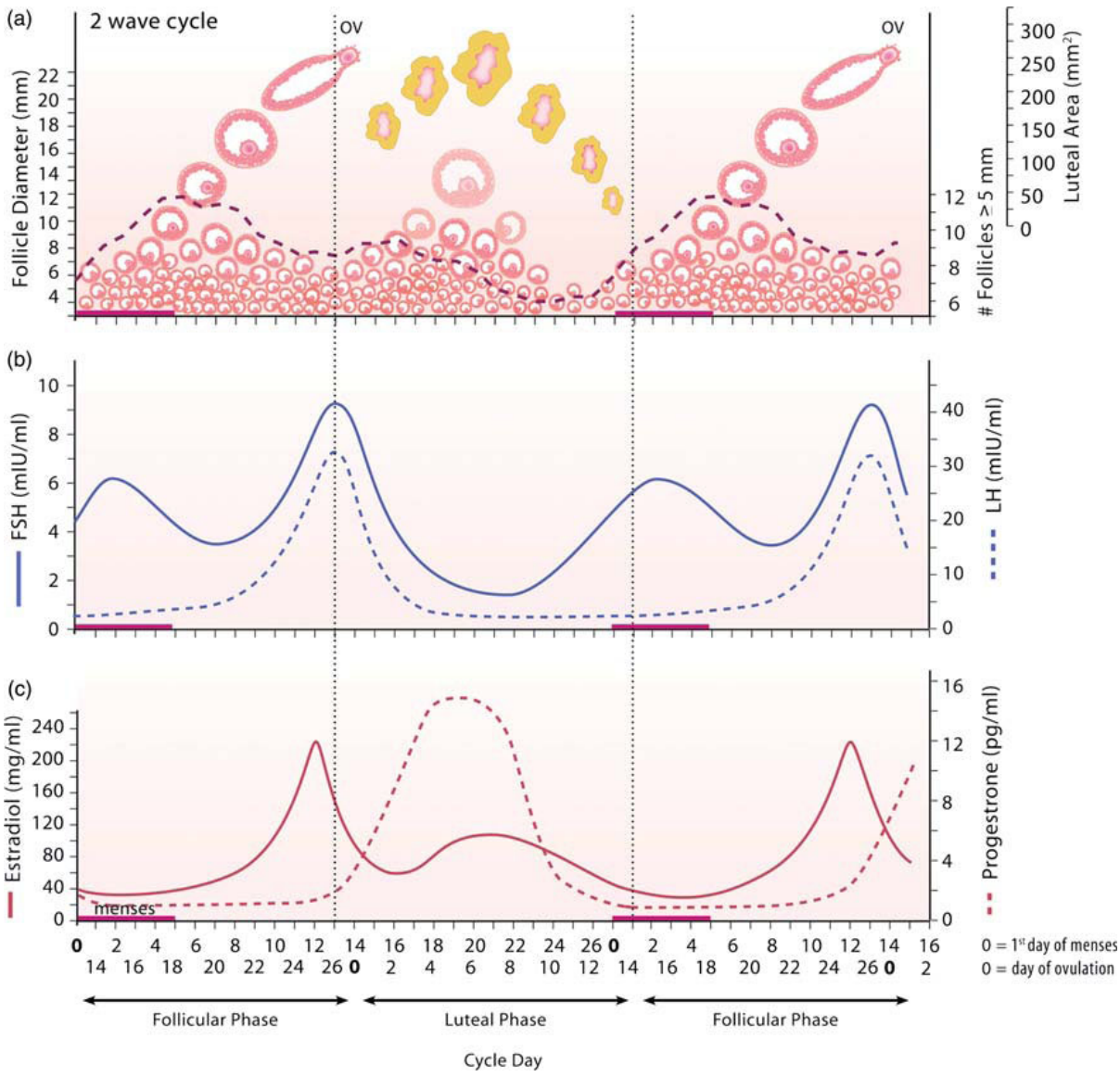

Figure 3.2 Graphs are taken from Baerwald et al. [Bae12], based on results from Baerwald et al. (2003a,b) [Bae03a; Bae03b]. Panel **(a)** depicts 2 follicle waves per cycle and the corpus luteum (yellow body). Panels **(b)** and **(c)** graph corresponding LH, FSH, E2, and P4 concentrations. Two-thirds of the women studied had cycles exhibiting 2 follicle waves per cycle and their results are shown. Note that 2 follicle waves per cycle corresponds to 2 rises in FSH. From A.R. Baerwald, G.P. Adams, and R.A. Pierson, Ovarian antral folliculogenesis during the human menstrual cycle: a review, *Human Reproduction Update*, 2012, volume 18, issue 1, pages 73-91 by permission of Oxford University Press. *Human Reproduction Update* is published on behalf of the European Society of Human Reproduction and Embryology (ESHRE).

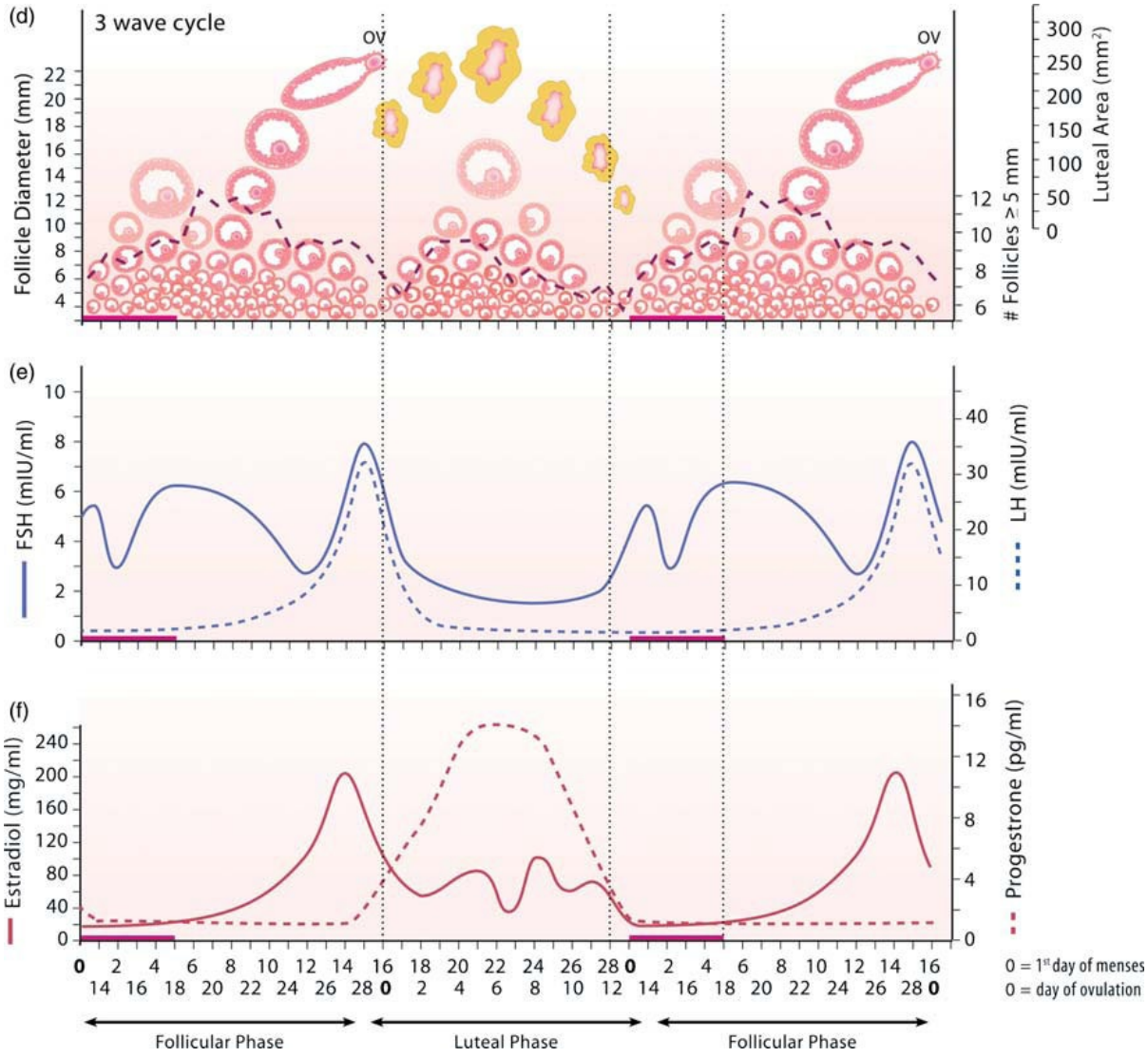

Figure 3.3 Graphs are taken from Baerwald et al. [Bae12], based on results from Baerwald et al. (2003a,b) [Bae03a; Bae03b]. Panel **(d)** depicts 3 follicle waves per cycle and the corpus luteum (yellow body). Panels **(e)** and **(f)** graph corresponding LH, FSH, E2, and P4 concentrations. One-third of the women studied had cycles exhibiting 3 follicle waves per cycle and their results are shown. Note that 3 follicle waves per cycle corresponds to 3 rises in FSH. From A.R. Baerwald, G.P. Adams, and R.A. Pierson, Ovarian antral folliculogenesis during the human menstrual cycle: a review, *Human Reproduction Update*, 2012, volume 18, issue 1, pages 73-91 by permission of Oxford University Press. *Human Reproduction Update* is published on behalf of the European Society of Human Reproduction and Embryology (ESHRE).

In this study, we illustrate follicle waves in normally cycling women by modifying the mathematical model introduced in Harris' thesis [Har01] and Harris-Clark *et al.*, 2003 [HC03], which consists of 13 nonlinear, delay differential equations. We alter this system by including a single FSH threshold function to stimulate the growth of the first stage of follicular development as suggested by Zeleznik [Zel04]. With a FSH threshold, the follicular phase rise in FSH and the mid-cycle surge in FSH will both promote the development of dominant follicles and the possibility of dual ovulations. To prevent a second dominant follicle, we add follicle atresia which depends on LH and this suppresses the development of a dominant follicle stage during the luteal phase. In her thesis, Margolskee [Mar13] was the first to experiment with FSH thresholds and atresia and to demonstrate the possibility of follicle waves in a mathematical model.

The parameters of our system of differential equations are estimated here using the data of McLachlan *et al.* [McL90a]. These data resemble the Baerwald hormone profiles in Figure 3.2 but also include inhibin A which is needed in our model because of its effect on FSH synthesis (see Section 3.2.1). Simulations of our model approximate well the pituitary and ovarian hormone profiles in McLachlan *et al.* [McL90a]. Also, simulations of the different stages of follicle development exhibit a follicle wave resulting in a dominant follicle during the follicular phase and a second wave of nonovulatory follicles during the early luteal phase similar to those depicted in Figure 3.2, Panel (a). Numerical experiments are carried out to show that this model may also produce three follicle waves per cycle. In particular, we input a FSH profile similar to that in Panel (e) of Figure 3.3 to illustrate that our model can produce three follicle waves like those in Panel (d) of Figure 3.3.

An interesting biological question is what conditions permit an ovulation from the second follicle wave and, hence, the possibility of fertilization of two ova at different times during the same menstrual cycle. The occurrence of dizygotic twins [Hal03] in such a case is referred to as superfecundation [Jam80; Wen92]. Our model may be used to illustrate the possibility of superfecundation. By removing the atresia term and making some other parameter modifications, we show that the second follicle wave can result in a second dominant follicle which will elicit a second LH surge and another ovulation.

3.2 Model Development

Many mathematical models for hormonal control of the menstrual cycle track blood levels of hormones produced by the brain and the ovaries during the follicular and luteal phases of the cycle using systems of differential equations. Our model is based on a nonlinear system of 13 delay, differential equations first presented in Harris-Clark *et al.* [HC03] which includes the five reproductive hormones LH, FSH, E2, P4, and InhA. Model parameters are estimated using data for 33 normally cycling women in McLachlan *et al.* [McL90a] which provides average daily blood levels of the 5 hormones over a 31 day month. Because the ovaries respond to daily averages (Odell [Ode79]),

our model lumps the effects of the hypothalamus and the pituitary together and we consider ovarian hormone regulation of the synthesis and release of FSH and LH on a time scale of days (see Section 3.2.1). In addition, because the clearance of the ovarian hormones from the blood is rapid compared to the clearance of the pituitary hormones and compared to the time scale for ovarian development, we assume that the blood levels of the ovarian hormones are at quasi-steady state [Kee09]. Hence, their concentrations are expressed as linear combinations of ovarian stages of the cycle (see Section 3.2.2). These simplifications permit the use of a daily time scale to track hormonal variation during the cycle. Finally, similar to the approach of Harris-Clark *et al.* [HC03], we construct our model in three steps: a pituitary system, an ovarian system, and the full system.

3.2.1 The Pituitary System

Four differential equations are used to represent the synthesis, release, and clearance of LH and FSH from the pituitary into the blood under control of the ovarian hormones (Figure 3.4). These equations were derived in Schlosser and Selgrade [Sch00] where the state variables, RP_{LH} and RP_{FSH}, represent the amounts of LH and FSH in the pituitary reserve pool and the state variables, LH and FSH, represent concentrations in the blood. Assuming V is constant blood volume, the four equations take the general form:

$$\frac{d}{dt}RP_{LH} = \text{synth}_{LH} - \text{rel}_{LH} \tag{3.1}$$

$$\frac{d}{dt}LH = \frac{1}{V}\text{rel}_{LH} - \text{clear}_{LH} \tag{3.2}$$

$$\frac{d}{dt}RP_{FSH} = \text{synth}_{FSH} - \text{rel}_{FSH} \tag{3.3}$$

$$\frac{d}{dt}FSH = \frac{1}{V}\text{rel}_{FSH} - \text{clear}_{FSH} \tag{3.4}$$

Synthesis and release rates for LH and FSH are described as rational functions of ovarian hormones in which stimulatory effects appear in the numerators and inhibitory effects appear in the denominators. Clinical research has indicated that P4 stimulates the release of LH and FSH into circulation (see [Cha78]) and that low levels of E2 inhibit the release of LH and FSH (see [Tsa71]). Also, it has been shown [Liu83; Yen05] that the high levels of E2 produced by the dominant follicle elicit the mid-cycle LH surge, so the numerator of the LH synthesis term contains a Hill function of E2 to reflect this effect on LH. The inhibins inhibit FSH synthesis [Yen05].

These features are discussed in detail in Schlosser and Selgrade [Sch00] and Harris-Clark *et al.* [HC03] where the following system expands eqs.(3.1)-(3.4):

$$\frac{d}{dt}RP_{LH} = \frac{v_{0LH} + \dfrac{v_{1LH}\,E_2(t-d_E)^a}{Km_{LH}^a + E_2(t-d_E)^a}}{1+\dfrac{P_4(t-d_P)}{Ki_{LH,P}}} - \frac{k_{LH}(1+c_{LH,P}\,P_4)RP_{LH}}{1+c_{LH,E}\,E_2} \tag{3.5}$$

$$\frac{d}{dt}LH = \frac{1}{V}\,\frac{k_{LH}(1+c_{LH,P}\,P_4)RP_{LH}}{1+c_{LH,E}\,E_2} - a_{LH}\,LH \tag{3.6}$$

$$\frac{d}{dt}RP_{FSH} = \frac{v_{FSH}}{1+\dfrac{InhA(t-d_{InhA})}{Ki_{FSH,InhA}}} - \frac{k_{FSH}(1+c_{FSH,P}\,P_4)RP_{FSH}}{1+c_{FSH,E}\,E_2^2} \tag{3.7}$$

$$\frac{d}{dt}FSH = \frac{1}{V}\,\frac{k_{FSH}(1+c_{FSH,P}\,P_4)RP_{FSH}}{1+c_{FSH,E}\,E_2^2} - a_{FSH}\,FSH \tag{3.8}$$

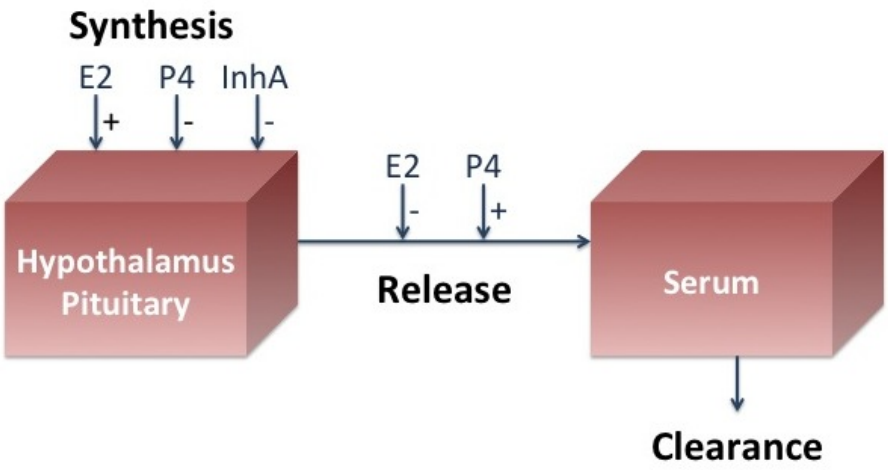

Figure 3.4 The brain and the blood compartments for the pituitary model are illustrated. E2, P4, and InhA stimulate (+) and/or inhibit (-) the synthesis and/or release of the pituitary hormones. Clearance from the blood is linear.

The data of McLachlan *et al.* [McL90a] for the ovarian hormones are used to obtained statistical fits for input functions $E_2(t)$, $P_4(t)$, and $InhA(t)$ in eqs.(3.5)-(3.8). Thus, in this step of the modeling process, eqs.(3.5)-(3.8) are time-dependent ordinary differential equations which are linear in the state variables, RP_{LH}, LH, RP_{FSH} and FSH. The parameters d_E, d_P, and d_{InhA} denote the period

of time between when changes in E2, P4, InhA blood levels occur and changes in the synthesis rates of LH and FSH result. These time-delays are used only in the synthesis terms because we assume that hormone synthesis is a more complicated biological process than hormone release. Then the data of McLachlan *et al.* [McL90a] for LH and FSH are used to estimate the 16 unknown parameters of eqs.(3.5)-(3.8) as was done in Harris-Clark *et al.* [HC03].

3.2.2 The Ovarian System

The ovarian model, first developed by Selgrade and Schlosser [Sel99], describes nine stages in the monthly growth and development of the ovaries. FSH and LH promote the growth of follicular tissue within a stage and the transfer of follicular tissue from one stage to the next. The capacity to produce hormones at each stage of the cycle is assumed to be proportional to the mass of the ovarian follicles or corpus lutea at that stage. The nine stages are:

- (RcF) Recruited Stage: FSH induced recruitment from the preantral pool
- (GrF) Growing Stage: FSH sustaining growth of cohort
- ($DomF$) Dominant Stage: Selection of a dominant follicle
- (OvF_1) First Ovulatory Stage: Follicle ovulation
- (OvF_2) Second Ovulatory Stage: Follicle luteinization
- (Lut_{1-4}) Luteal Stages: Four stages of corpus luteum decay.

The increase of mass and transfer of mass for each stage is described by a differential equation which is linear in the state variables with coefficients depending on the pituitary hormones. A transfer term in one equation appears as a growth term in the next equation as follows.

$$\frac{d}{dt}RcF = b \cdot FSH + \frac{c_1 FSH^p}{Km_F^p + FSH^p} RcF - c_2 LH^\alpha RcF \tag{3.9}$$

$$\frac{d}{dt}GrF = c_2 LH^\alpha RcF + (c_3 LH^\beta - c_4 LH) GrF \tag{3.10}$$

$$\frac{d}{dt}DomF = c_4 LH \cdot GrF - c_5 LH^\gamma DomF - \frac{c_{atr} DomF}{1 + (LH/Ki_{atr})^q} \tag{3.11}$$

$$\frac{d}{dt}OvF_1 = c_5 LH^\gamma DomF - d_1 OvF_1 \tag{3.12}$$

$$\frac{d}{dt}OvF_2 = d_1 OvF_1 - d_2 OvF_2 \tag{3.13}$$

$$\frac{d}{dt}Lut_1 = d_2 OvF_2 - k_1 Lut_1 \tag{3.14}$$

$$\frac{d}{dt}Lut_2 = k_1 Lut_1 - k_2 Lut_2 \tag{3.15}$$

$$\frac{d}{dt}Lut_3 = k_2 Lut_2 - k_3 Lut_3 \tag{3.16}$$

$$\frac{d}{dt}Lut_4 = k_3 Lut_3 - k_4 Lut_4 \tag{3.17}$$

Applying the quasi-steady state assumption as did Bogumil *et al.* [Bog72a; Bog72b], we write ovarian hormone concentrations as linear combinations of the stages that secrete these hormones:

$$E_2 = e_0 + e_1 GrF + e_2 DomF + e_3 Lut_4 \tag{3.18}$$

$$P_4 = p_0 + p_1 Lut_3 + p_2 Lut_4 \tag{3.19}$$

$$InhA = h_0 + h_1 DomF + h_2 Lut_2 + h_3 Lut_3 + h_4 Lut_4 \tag{3.20}$$

The ovarian system of previous models [Sel99; HC03; Sel09; Mar11] used first order FSH terms to initiate follicular growth. However, Zeleznik (2004) [Zel04] suggests that FSH levels must exceed a threshold to initiate follicular development. Such a threshold effect may be captured mathematically using the Hill function of FSH in eq.(3.9):

$$\frac{c_1 FSH^p}{Km_F^p + FSH^p}.$$

This function of FSH has an increasing sigmoidal shaped graph. The Hill coefficient p determines the steepness of the graph, the parameter c_1 is the limiting value of the function, and the half-saturation parameter Km_F is the FSH value giving a function value of $0.5\,c_1$. Here we show that parameters may be found so that this single Hill function as it appears in the differential equation (3.9) results in the appearance of two follicle waves.

For a normally cycling woman, only the wave occurring in the follicular phase will result in an ovulating follicle. To prevent a second dominant follicle, we add follicle atresia in eq.(3.11) which depends inversely on LH:

$$\frac{c_{atr}\,DomF}{1+(LH/Ki_{atr})^q}.$$

Because luteal P4 inhibits LH synthesis, LH is low during the luteal phase resulting in a larger atresia term. Hence a luteal phase follicle wave does not produce a dominant follicle and no second ovulation occurs. In Section 3.5, we show that the removal of this atresia term does result in a second ovulation and the possibility of fraternal twins.

In eqs.(3.9)-(3.17), $FSH(t)$ and $LH(t)$ are explicit functions of time t obtained statistically from the pituitary hormone data of McLachlan *et al.* [McL90a]. Then the McLachlan data for E2, P4, and InhA are used to estimate the 32 parameters in eqs.(3.9)-(3.20) as was done in Section 3.2.1.

3.2.3 The Merged System

The third and final step of model construction is to merge the pituitary system and ovarian system together to create a single 13-dimensional system of differential equations (3.5)-(3.17) with three auxiliary equations (3.18)-(3.20). The nonlinear coefficient functions of the inputs in Sections 3.2.1 and 3.2.2 now become nonlinear functions of state variables so the system is highly nonlinear. The parameters d_E, d_P, and d_{InhA} are discrete time-delays so (3.5)-(3.17) are delay differential equations. The 51 parameters of (3.5)-(3.20) must be re-estimated using the data of McLachlan *et al.* [McL90a] but the parameters found in Sections 3.2.1 and 3.2.2 are good starting values. Optimized parameters are obtained using least squares and the Nelder-Mead Simplex method implemented in MATLAB [Nel65] (see Panza [Pan01] for details). These parameters are listed in Table 3.1.

3.3 Model Simulations – Two Follicle Waves

Numerical solutions to eqs.(3.5)-(3.20) are computed using the delay equations solver DDE23 in MATLAB. Testing a variety of initial conditions indicates that solutions approach a unique stable solution of period approximately 31.5 days. Initial conditions for this stable cycle are listed in Table 3.2 and are used to plot the follicle stages for two complete cycles in Figure 3.5 and the four hormones LH, FSH, E2, and P4 against the data of McLachlan *et al.* [McL90a] in Figures 3.6 and 3.7. The left panel of Figure 3.5 displays the first 3 ovarian follicle stages, the recruited stage RcF, the growing stage GrF, and the dominant stage $DomF$. RcF and GrF exhibit two follicle waves – a large follicular phase wave which becomes the dominant, ovulatory follicle and a smaller luteal phase wave. The atresia term in eq.(3.11) eliminates a luteal phase dominant follicle. In fact, the atresia

is so successful at reducing the dominant stage after midcycle that all subsequent stages, OvF_1 through Lut_4, are quite small (see the right panel in Figure 3.5).

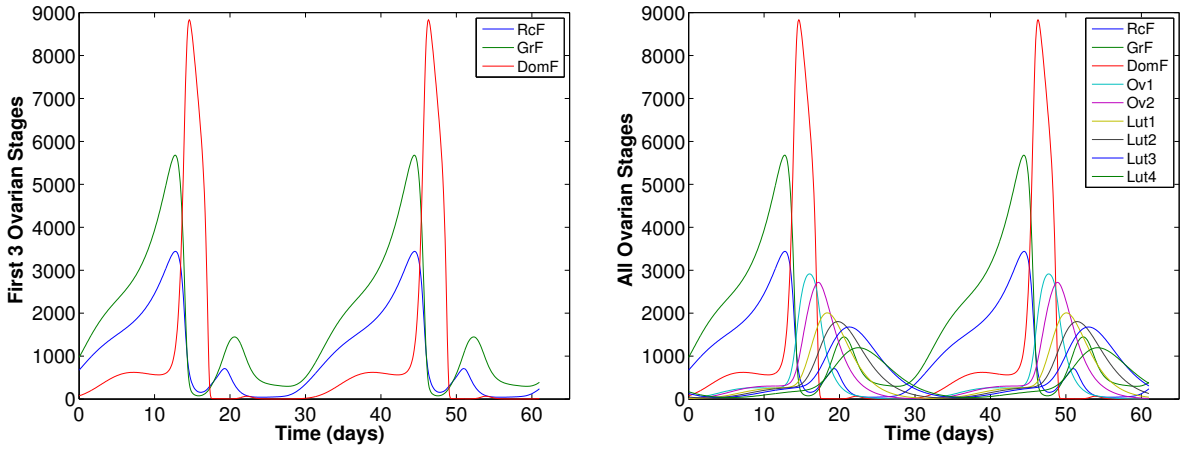

Figure 3.5 All ovarian follicle stages for the merged model eqs.(3.5)-(3.20) with parameters of Table 3.1 are shown for two cycles. The model maintains two follicle waves for the recruited RcF and growing GrF stages (left panel). The atresia term reduces the dominant stage DomF after midcycle and effectively results in small subsequent ovarian stages (right panel).

From eqs.(3.18)-(3.20) for the ovarian hormones, note that the second follicle wave affects only E2 and this is because of the GrF term in eq.(3.18). As a result, the luteal E2 peak is higher than the data and almost 80% of the follicular E2 peak (see Figure 3.6, left panel). Because E2 promotes LH synthesis, eq.(3.5), there is additional LH in the luteal phase appearing as a small bump in the LH profile (see Figure 3.7, left panel). P4, which depends on the luteal stages, does not reach the luteal data peak (see Figure 3.6, right panel) because these stages are small.

3.4 Three Follicle Waves

Baerwald et al. [Bae12] illustrated three follicle waves per cycle depicted in Figure 3.3, Panel (d). Each wave corresponds to a different peak in FSH as observed in Figure 3.3, Panel (e), where a late luteal rise in FSH is interrupted by an early follicular dip in the FSH graph followed by its normal follicular phase rise. Daily FSH data for such a FSH profile are not available for us to use in a full model simulation. However, in order to test if our model can generate three follicle waves from this type of FSH profile, we use the ovarian model component discussed and implemented in Section 3.2.2. An input function $LH(t)$ is obtained from the data of McLachlan *et al.* [McL90a] as done in Section 3.2.2 but a new input for $FSH(t)$ is defined using negative exponential functions of t to

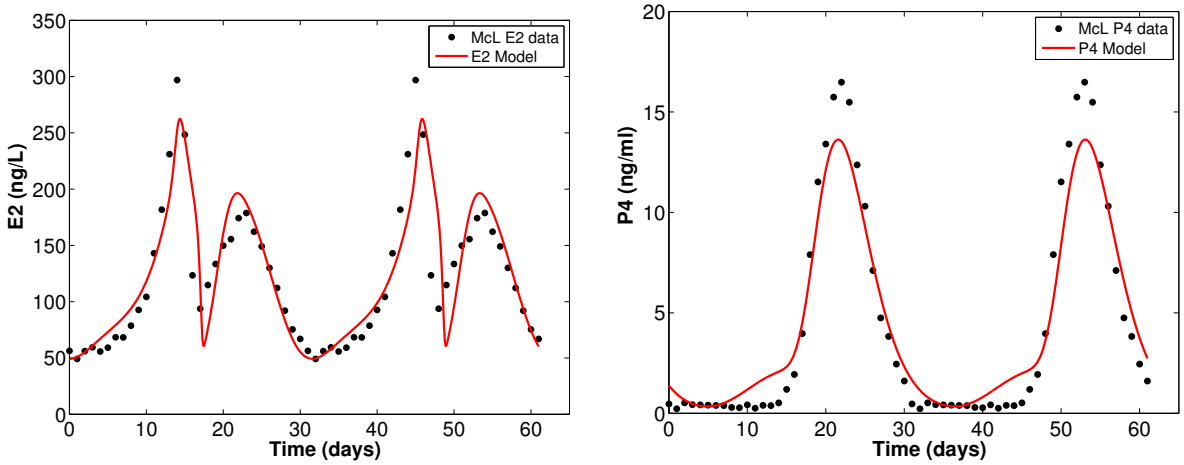

Figure 3.6 Ovarian hormones E2 and P4 for the merged model eqs.(3.5)-(3.20) with parameters of Table 3.1 are plotted against the McLachlan data [McL90a] for two cycles.

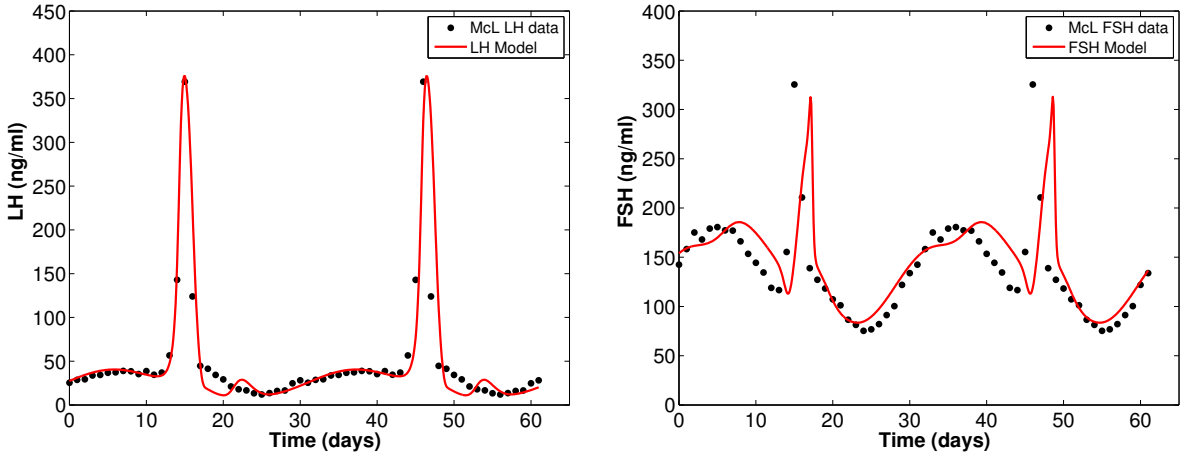

Figure 3.7 Pituitary hormones LH and FSH for the merged model eqs.(3.5)-(3.20) with parameters of Table 3.1 are plotted against the McLachlan data [McL90a] for two cycles.

position three appropriately spaced rises as follows:

$$FSH = 82.5 + 190e^{-\frac{(t-8)^2}{10}} + 180e^{-\frac{(t-0.3)^2}{0.4}} + 400e^{-\frac{(t-15.2)^2}{3}} - 20e^{-\frac{(t-24)^2}{15}}. \qquad (3.21)$$

This FSH profile is scaled to be consistent with the McLachlan data and is plotted in Figure 3.8.

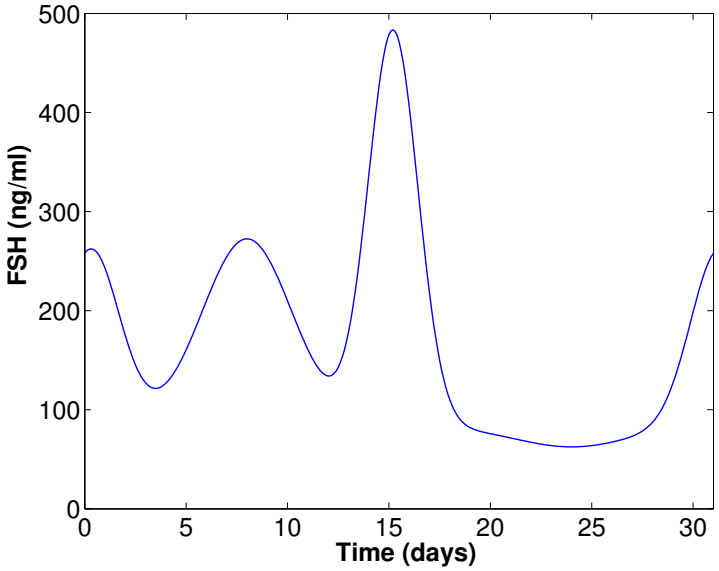

Figure 3.8 The FSH input function (3.21) has three distinct rises during one cycle and is used to produce three follicle waves.

These input functions for $LH(t)$ and $FSH(t)$ are inserted into the system of differential equations (3.9)-(3.17) with auxiliary equations (3.18)-(3.20) to produce three follicle waves per cycle (Figure 3.9). The data for E2, P4, and InhA from McLachlan *et al.* [McL90a] are used to optimize the parameters (see Panza [Pan01] for details) and these parameters are listed in Table 3.3. Figure 3.10 plots model simulations of the ovarian hormones against the data of McLachlan *et al.* [McL90a]. Notice that three waves occur for the first two ovarian stages RcF and GrF but the atresia term eliminates the first and third waves in the dominate stage (Figure 3.9, left panel). To prevent an early follicular rise in E2 (Figure 3.10), we reduce the parameter e_1 in eq.(3.18) to one-half of its value for the two wave model (compare Tables 3.1 and 3.3).

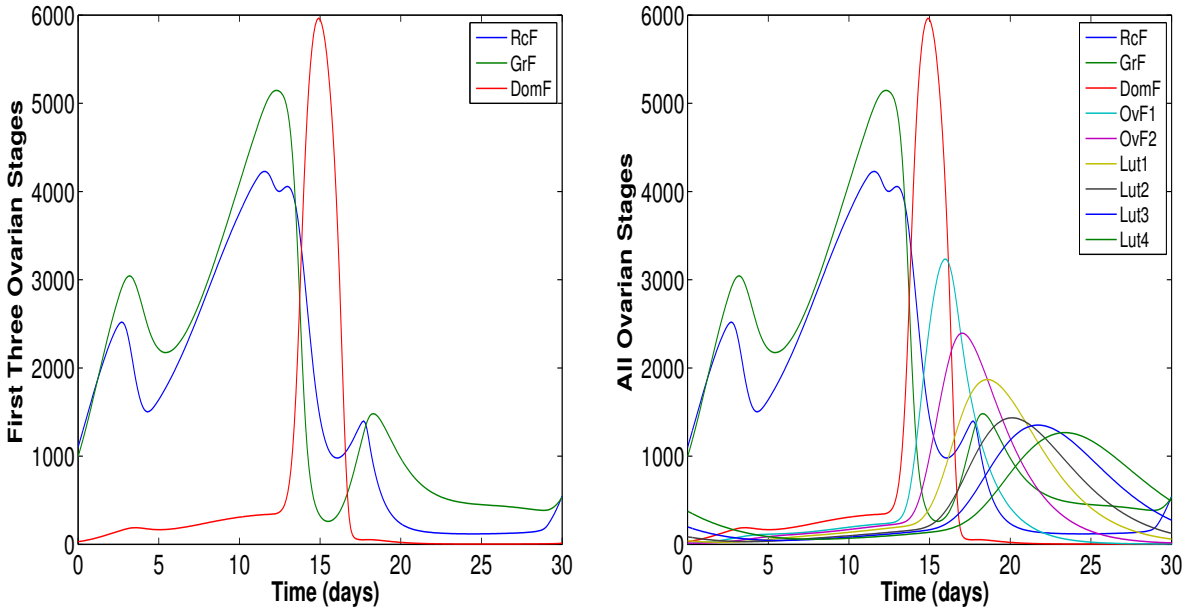

Figure 3.9 Follicle stages are plotted for eqs.(3.9)-(3.20) where the FSH input (3.21) has three distinct rises. The parameters are given in Table 3.3. The left panel depicts the first three stages of follicle growth and isolates waves in the recruited RcF (-) and the growing GrF (-) stages. Note that DomF (-) exhibits only one wave. The right panel gives the complete set of nine follicle stages.

3.5 Superfecundation

Dizygotic twinning may happen when multiple ovulations occur during a single or consecutive menstrual cycles and two oocytes are fertilized [Hal03]. In recent years, the incidence of this has increased partially due to more women receiving fertility treatments and more older women becoming pregnant [Bor99; Wes97]. Though rare, dizygotic twins via superfecundation could be a direct consequence of multiple follicle waves per cycle. Superfecundation is the ovulation and fertilization of two oocytes at different times during the same menstrual cycle [Jam80]. This may occur if two follicle waves result in two dominant, ovulatory follicles during the same cycle. Most cases of superfecundation are noticed only when the twins have different fathers because they look drastically different or by chance a paternity test is conducted. A recent child support case was deemed 'groundbreaking' because the paternity test on twins showed that they had different fathers and the father who was being sued only had to pay support for one of the twins [Mue15].

Here we show that removing the atresia term from eq.(3.11) and changing some parameters cause a luteal phase dominant follicle which secretes enough E2 to elicit a second LH surge and a second ovulation. If both oocytes are fertilized then dizygotic twins may result. First, setting the parameter c_{atr} to zero removes the atresia term in eq.(3.11). This permits the growth of a dominant follicle stage during the luteal phase (Figure 3.11) and the resulting secretion of large amounts of

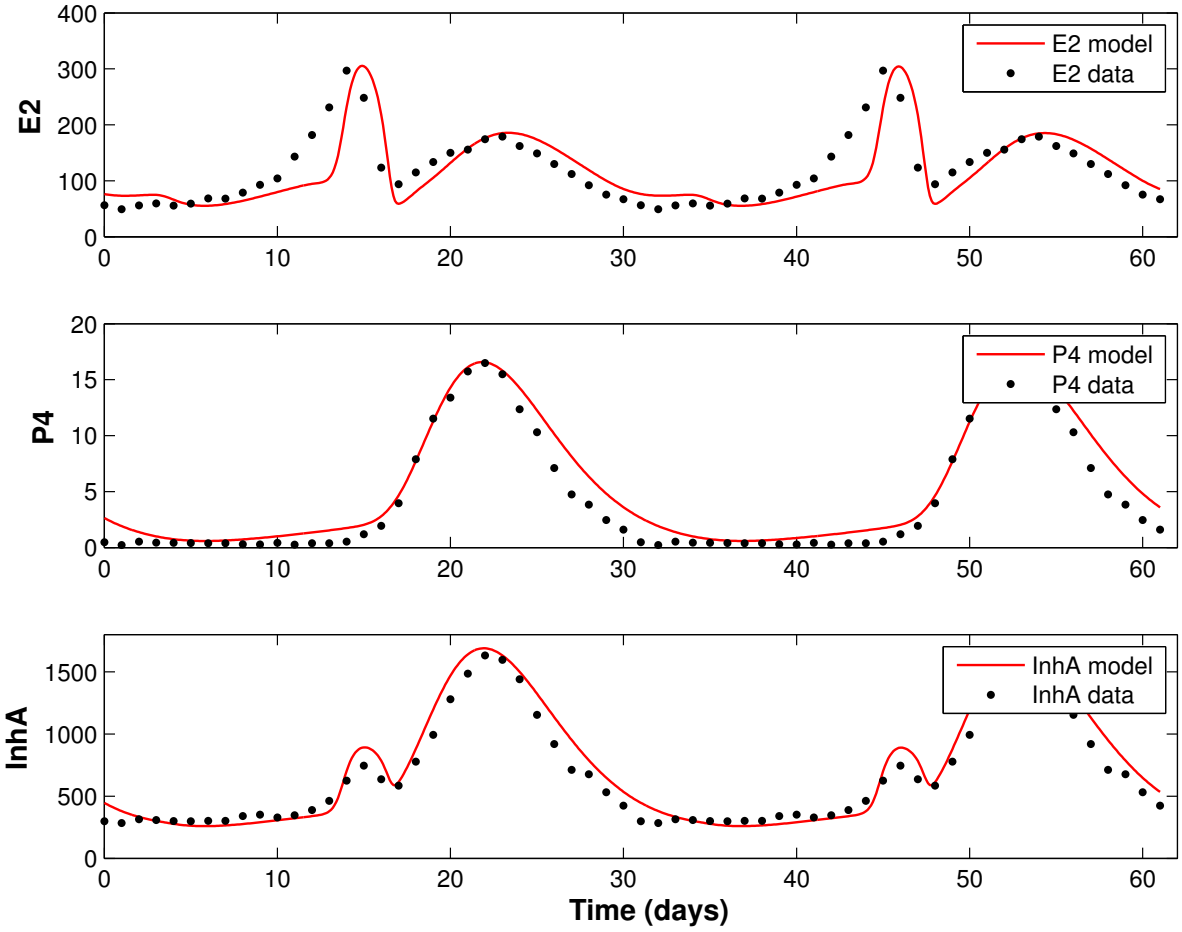

Figure 3.10 The data of McLachlan *et al.* [McL90a] for the ovarian hormones is compared to simulations of eqs.(3.9)-(3.20) with parameters of Table 3.3. The FSH input function (3.21) with three distinct rises is used.

luteal E2 (Figure 3.12). E2 promotes the synthesis of LH but P4 inhibits LH (see the first term in eq. 3.5). To guarantee a luteal LH surge (Figure 3.12) we diminish luteal P4 via eq.(3.19) by decreasing parameter p_1 slightly and parameter p_2 by a factor of 10, (compare Table 3.1 and Table 3.4). Other *ad hoc* parameter adjustments are made to insure two LH surges of comparable strength, e.g., v_{1LH} is increased and v_{0LH} is decreased. Then the data for FSH, E2, and InhA from McLachlan *et al.* [McL90a] are used to optimize remaining parameters (see Panza [Pan01] for details).

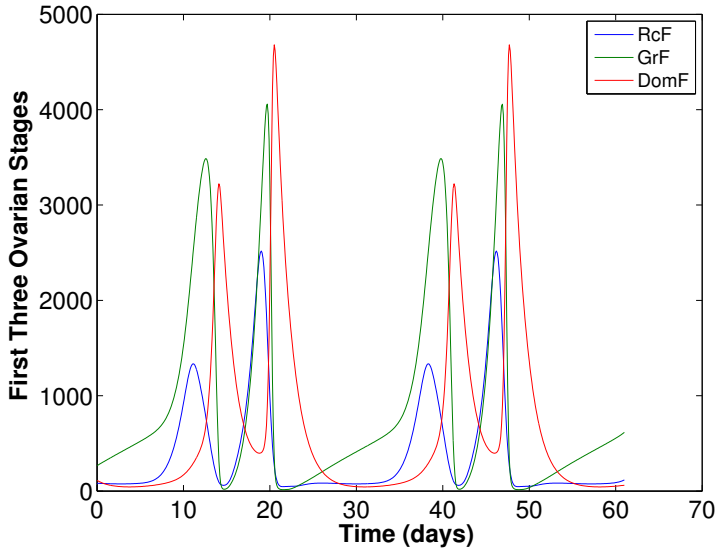

Figure 3.11 The first 3 stages of ovarian development for the model of follicle wave superfecundation are plotted for two cycles. The parameters are given in Table 3.4. The luteal phase DomF (-) stage produces large amounts of luteal E2 which causes a second LH surge, Figure 3.12.

3.6 Sensitivity and Bifurcation Analyses

Sensitivity analysis measures changes in system behavior with respect to changes in parameters [Yue06]. The purpose is to identify the parameters that have the largest impact on the dynamical behavior of the system. The parameters that greatly affect the model output when changed slightly are known as sensitive parameters while the parameters that have little effect on the model output are known as insensitive parameters [Pop09]. Local sensitivity analysis examines the effects the system undergoes when each parameter is changed one at a time. Here model outputs of crucial importance are the follicular phase E2 peak because it affects the LH surge and the FSH profile because it determines the follicle waves. So Panza [Pan01] computes a normalized sensitivity coefficient for each model parameter measuring changes in E2 for four days centered at the E2 peak (ranked in

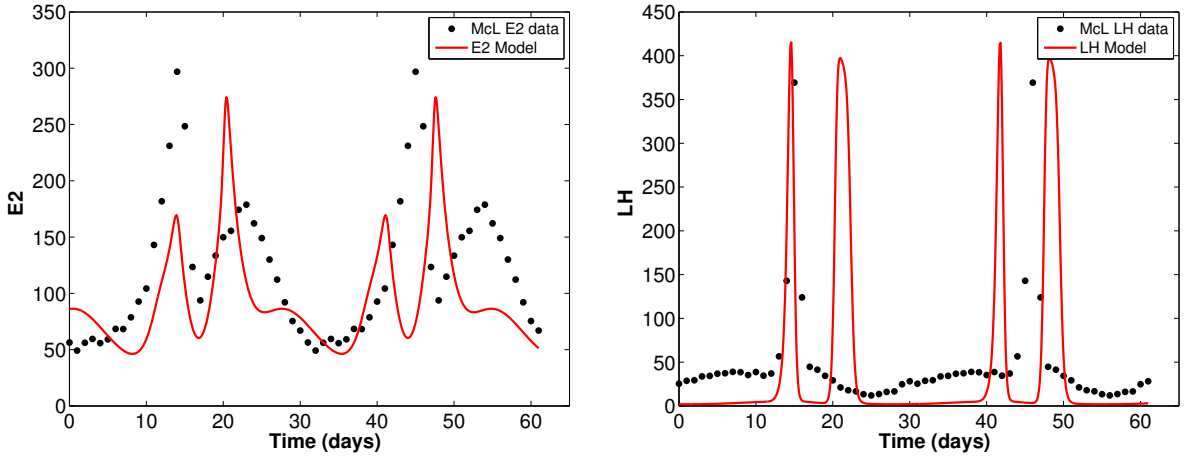

Figure 3.12 E2 and LH from the model of follicle wave superfecundation is compared to the McLachlan data [McL90a] for two cycles. During one cycle, a second LH surge is present due to increased luteal E2 levels produced by a second dominant follicle. A second LH surge allows for ovulation of the second dominant follicle for potential fertilization resulting in superfecundation.

Table 3.5, column 2) and another coefficient for changes in FSH for one complete cycle (ranked in Table 3.5, column 3). The five most sensitive parameters are ranked in Table 3.5 with v_{FSH} being the most sensitive for both model outputs. Notice that the five most sensitive parameters are the same for both outputs. The parameters v_{FSH}, v_{0LH}, and Km_{LH} affect the synthesis of the pituitary hormones, which control ovarian development. Km_F is the half-satuation for the Hill function which promotes the growth of the first follicle stage RcF and α affects the transfer of mass from RcF to GrF (see eq.(3.9)). These two are the stages which exhibit follicle wave behavior.

Numerical simulations of eqs.(3.5)-(3.20) with parameters from Table 3.1, which were optimized using the data of McLachlan *et al.* [McL90a], indicate that the stable cycle is unique (Figures 3.6 and 3.7). If the sensitive parameters in Table 3.5 are varied near their best-fit values, the unique stable cycle appears to persist. Using the bifurcation software for delay differential equations, DDEBIFTOOL [Eng00], confirms this suspicion by displaying a simple continuation curve through the best-fit value and no bifurcations nearby (see Figure 3.13 for the parameter Km_F). Hence, a woman whose reproductive cycle is determined by this parameter set would cycle normally and small perturbations would not significantly disturb her cycle.

The superfecundation system, eqs.(3.5)-(3.20) with parameters from Table 3.4, produces dominant follicles $DomF$ in both the follicular and luteal phases of the cycle primarily because of the absence of atresia. Introducing atresia by permitting the atresia coefficient c_{atr} to be nonzero and by taking $q = 2.36$ and $Ki_{atr} = 4.69$ results in interesting dynamical behavior. Increasing c_{atr} diminishes the dominant follicle and the LH surge during the follicular phase but not the luteal phase (Figure 3.14). For c_{atr} near 20, the follicular phase LH surge is clearly too small to cause

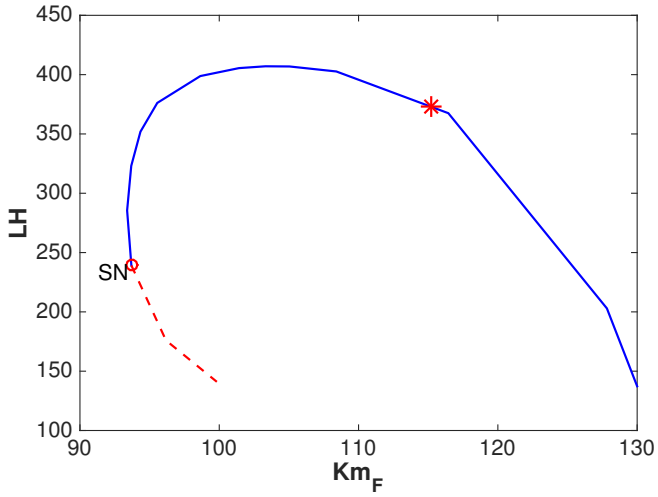

Figure 3.13 This bifurcation diagram plots the maximal LH value along a periodic solution of eqs.(3.5)-(3.20) against Km_F with the remaining parameters from Table 3.1. SN denotes a saddle-node bifurcation and the $*$ indicates the position of the cycle for best-fit $Km_F = 115.18$. The solid blue curve represents stable cycles and the dashed red curve, unstable cycles.

ovulation so ovulation occurs only during the luteal phase and the possibility of superfecundation is lost. For a woman whose cycle is described by this situation, her cycle length is normal (here about 30 days) but ovulation occurs much later than mid-cycle. Observe the LH profile in Figure 3.15, left panel, where the LH surge occurs at day 19 instead of day 15.

As c_{atr} increases above 20, a cascade of period-doubling bifurcations occurs. At $c_{atr} \approx 22.654$, the cycle of period 30 days becomes unstable and a stable cycle of about 60 days appears as observed by comparing the LH profiles for $c_{atr} = 22.6517$ and $c_{atr} = 22.7841$ (Figure 3.15). Then at $c_{atr} \approx 22.785$, a second period-doubling bifurcation occurs and a stable cycle of approximately 120 days appears. A portion of the bifurcation diagram showing these two period-doubling bifurcations is drawn in Figure 3.16.

The sequence of bifurcations as c_{atr} increases from 22.5 to 23 resembles the standard period-doubling route to chaos [Dev92] with a chaotic cycle at $c_{atr} = 22.85$ and a period-6 window around $c_{atr} = 22.894$ (Figure 3.17). The left panel of Figure 3.17 plots a menstrual cycle which is not exactly periodic but there are 12 LH surges per year. The right panel of Figure 3.17 plots a stable cycle of period about 180 days which is roughly six times the period of the cycle at $c_{atr} = 22.6517$. Such a interval in a bifurcation diagram is referred to as a period-6 window. A woman whose reproductive cycle is represented by this parameter regime could experience unpredictable cycles. This indicates the the two models corresponding to the parameters of Table 3.1 or of Table 3.4 with atresia are quite different. The model corresponding to Table 3.1 depicts a normally cycling woman with hormone

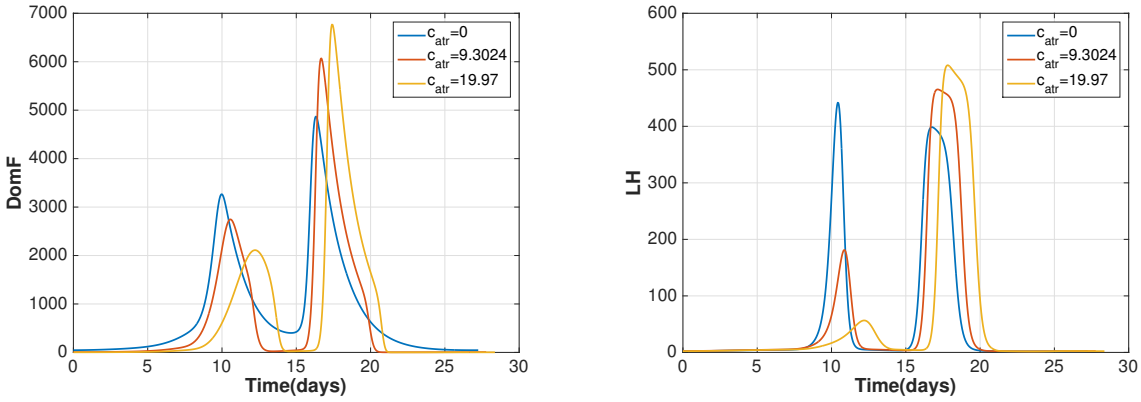

Figure 3.14 DomF and LH for the superfecundation model for three values of c_{atr} show a diminishing dominant follicle and LH surge during the follicular phase. If $c_{atr} \approx 20$, there is just one ovulation per cycle.

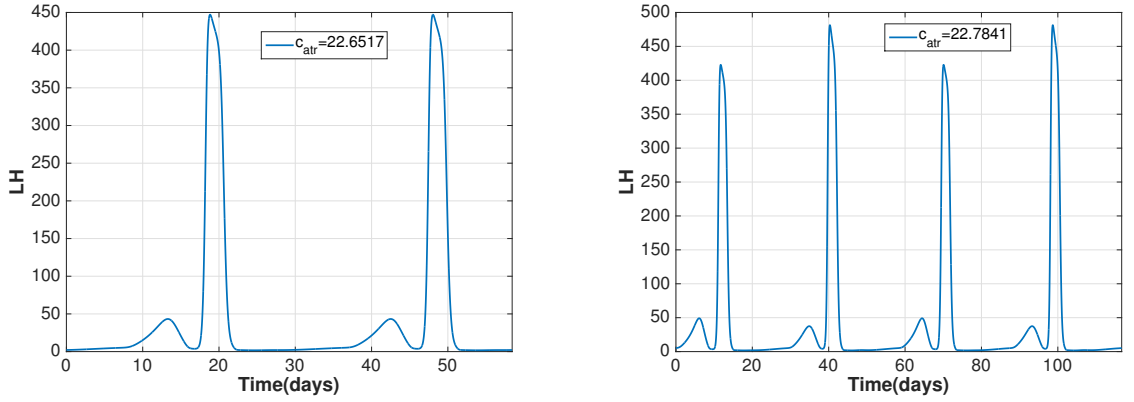

Figure 3.15 LH profiles for $c_{atr} = 22.6517$ and $c_{atr} = 22.7841$ illustrating that the period of the stable cycle doubles between these values, i.e., a period-doubling bifurcation occurs.

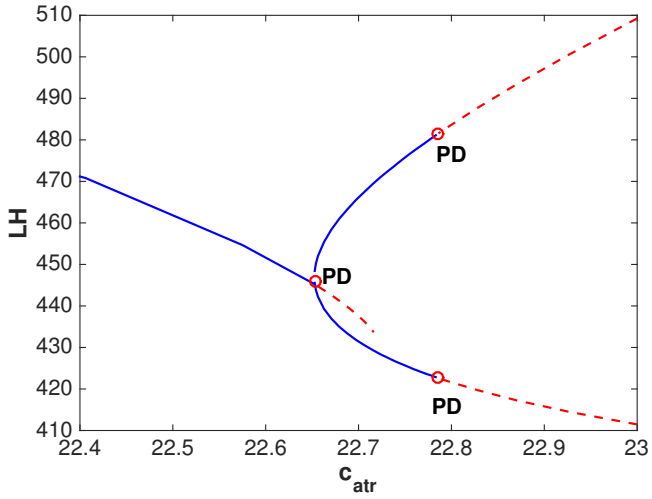

Figure 3.16 The maximal LH value along a periodic solution of eqs.(3.5)-(3.20) is plotted against c_{atr} with $q = 2.36$, $Ki_{atr} = 4.69$, and the remaining parameters from Table 3.4. PD denotes period-doubling bifurcations which occur at $c_{atr} \approx 22.654$ and $c_{atr} \approx 22.785$. The solid blue curves represent stable cycles and the dashed red curves, unstable cycles.

levels consistent with data in the literature [McL90a] and exhibiting two follicle waves per cycle. The model corresponding to Table 3.4 with atresia added represents a woman who may experience superfecundation but also whose cycle is easily disturbed by small variations in follicle atresia.

3.7 Summary and Discussion

This study describes a system of 13 nonlinear, delay differential equations with 51 parameters which models the phenomenon of follicle waves in normally cycling women first observed by Baerwald et al. [Bae03a; Bae03b; Bae12]. Using model eqs.(3.5)-(3.20), we exhibit menstrual cycles with two or three follicle waves corresponding to the number of rises in blood levels of FSH. Simulations with the parameters of Table 3.1 depict two follicle waves per cycle and resulting hormone profiles accurately approximate the data of McLachlan *et al.* [McL90a] (Figures 3.6 and 3.7). Data with three distinctive rises in FSH are not available but we use the input function plotted in Figure 3.8 with three FSH hills timed to correspond to the hills of Panel (e) in Figure 3.3 from Baerwald *et al.* [Bae12]. This input function in eqs.(3.9)-(3.20) with the parameters of Table 3.3 causes the formation of three follicle waves as depicted in Figure 3.9 and the resulting ovarian hormones are plotted against the data of McLachlan *et al.* [McL90a] in Figure 3.10. We conjecture that variations in InhB levels during the late luteal to early follicular transition might cause a FSH profile like Figure 3.3, Panel (e), but we do not have data to substantiate this conjecture. Since InhB inhibits FSH synthesis and is prominent during the late luteal to early follicular transition, decreases in InhB would result in increases in

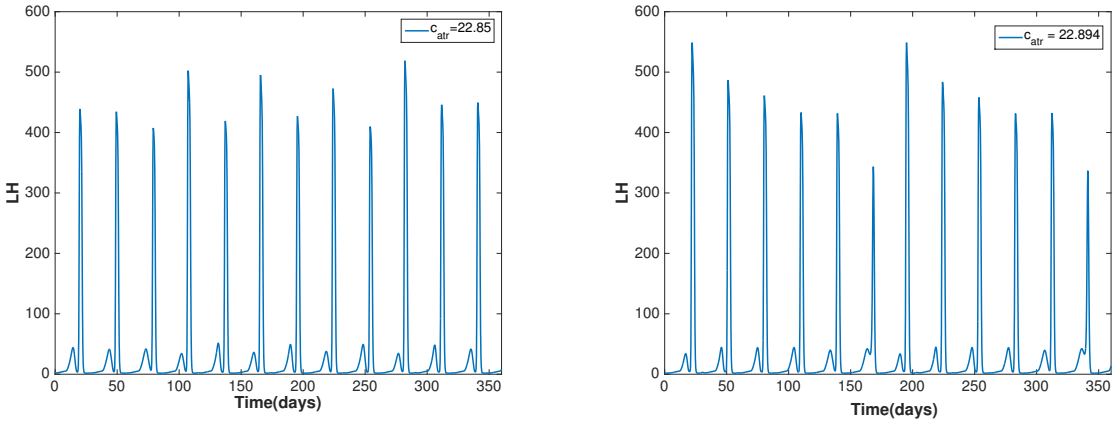

Figure 3.17 The left panel illustrates the LH profile of a stable, chaotic cycle at $c_{atr} = 22.85$. There are 12 LH surges per year but they do not have the same magnitude. The right panel plots the LH profile of a stable cycle of period approximately 180 days at $c_{atr} = 22.894$. This indicates the presence of a period-6 window in the c_{atr} bifurcation diagram.

FSH.

The inclusion of an atresia term in eq.(3.11) prevents more than one ovulation per cycle. We show that removing this term and making some parameter adjustments permit two ovulations per cycle and, hence, the possibility of dizygotic twins via superfecundation. Simulations of eqs.(3.5)-(3.20) with parameters of Table 3.4 exhibit two dominant follicles per cycle (Figure 3.11) and two LH surges (Figure 3.12, right panel). This situation results in two ovulations per cycle. Introducing atresia back into the superfecundation system by taking $q = 2.36$ and $Ki_{atr} = 4.69$ and increasing c_{atr} from zero, causes the loss of superfecundation and a cascade of period-doubling bifurcations. This system may produce erratic menstrual cycle behavior. Hence, although model equations are the same, the two models corresponding to the parameters of Table 3.1 or of Table 3.4 with atresia have different dynamical behavior and represent women with noticeably different reproductive hormone profiles.

Research on this project was made possible by a grant from the NSF and with help and guidance from Angela Baerwald.

Table 3.1 Parameters for the merged, two-wave model eqs.(3.5)-(3.20) fitting the McLachlan data [McL90a]. All of the following optimized parameters were truncated to two significant decimal digits.

Param.	**Value**	**Units**
a	11	dimensionless
V	2.5	L
a_{LH}	14	1/day
a_{FSH}	8.21	1/day
v_{0LH}	1577.78	μg/day
v_{1LH}	25,288.06	μg/day
Km_{LH}	228.65	ng/L
$Ki_{LH,P}$	3.01	μg/L
k_{LH}	12.26	1/day
$c_{LH,P}$	0.085	L/ μg
$c_{LH,E}$	9.22E-08	L/ng
d_E	0.47	days
d_P	0.80	days
v_{FSH}	5190.68	μg/day
$Ki_{FSH,InhA}$	654.11	U/L
k_{FSH}	12.83	1/day
$c_{FSH,P}$	2.46	L/ μg
$c_{FSH,E}$	0.0019	$(\text{L/ng})^2$
d_{InhA}	1.66	days
α	0.31	dimensionless
β	0.022	dimensionless
γ	0.011	dimensionless
b	0.60	L/day
c_1	1.59	1/day
c_2	0.51	$(\text{L}/\mu\text{g})^{\alpha}(1/\text{day})$
c_3	0.057	$(\text{L}/\mu\text{g})^{\beta}(1/\text{day})$

Param.	**Value**	**Units**
c_4	0.025	$(\text{L}/\mu\text{g})(1/\text{day})$
c_5	0.30	$(\text{L}/\mu\text{g})^{\gamma}(1/\text{day})$
d_1	0.70	1/day
d_2	0.59	1/day
k_1	0.66	1/day
k_2	0.63	1/day
k_3	0.60	1/day
k_4	0.80	1/day
Km_F	115.18	μg/L
p	19.80	dimensionless
c_{atr}	615.89	1/day
Ki_{atr}	4.69	μg/L
q	2.36	dimensionless
e_0	0.00	ng/L
e_1	0.023	1/kL
e_2	0.025	1/kL
e_3	0.14	1/kL
p_0	0.00	μg/L
p_1	0.0063	1/L
p_2	0.0025	1/L
h_0	208.76	U/L
h_1	0.0040	(U/L)/ μg
h_2	0.00	(U/L)/ μg
h_3	0.66	(U/L)/ μg
h_4	0.00098	(U/L)/ μg

Table 3.2 Initial conditions for the two-wave merged model eqs.(3.5)-(3.20) used for simulations plotted in Figures 3.5, 3.6, and 3.7.

State	**Value**	**Units**
$RP_{\mathrm{LH}}(0)$	83.43	μg
LH(0)	25.34	μg/L
$RP_{\mathrm{FSH}}(0)$	442.29	μg
FSH(0)	142.50	μg/L
$RcF(0)$	790.68	μg
$GrF(0)$	1160.43	μg
$DomF(0)$	113.01	μg
$OvF_1(0)$	24.77	μg
$OvF_2(0)$	15.19	μg
$Lut_1(0)$	14.94	μg
$Lut_2(0)$	37.76	μg
$Lut_3(0)$	104.52	μg
$Lut_4(0)$	140.12	μg

Table 3.3 Parameters for the three-wave ovarian component model eqs.(3.9)-(3.20) fitting the McLachlan data [McL90a]. All of the following optimized parameters were truncated to two significant decimal digits.

Parameter	**Value**	**Units**
α	0.31	dimensionless
β	0.20	dimensionless
γ	0.035	dimensionless
b	1.86	L/day
c_1	1.31	1/day
c_2	0.42	$(L/\mu g)^{\alpha}(1/day)$
c_3	0.14	$(L/\mu g)^{\beta}(1/day)$
c_4	0.035	$(L/\mu g)(1/day)$
c_5	0.39	$(L/\mu g)^{\gamma}(1/day)$
d_1	0.59	1/day
d_2	0.56	1/day
k_1	0.56	1/day
k_2	0.63	1/day
k_3	0.60	1/day
k_4	0.58	1/day
Km_F	122.10	μg/L
p	19.09	dimensionless
c_{atr}	285.45	1/day
Ki_{atr}	8.58	μg/L
q	1.83	dimensionless
e_0	16.00	ng/L
e_1	0.01	1/kL
e_2	0.045	1/kL
e_3	0.13	1/kL
p_0	0.00	μg/L
p_1	0.011	1/L
p_2	0.001	1/L
h_0	188.05	U/L
h_1	0.087	$(U/L)/(\mu g)$
h_2	0.01	$(U/L)/(\mu g)$
h_3	0.95	$(U/L)/(\mu g)$
h_4	0.18	$(U/L)/(\mu g)$

Table 3.4 Superfecundation parameters for the merged, two-wave model fitting the McLachlan data [McL90a]. All of the following optimized parameters were truncated to two significant decimal digits.

Param.	**Value**	**Units**
a	11	dimensionless
V	2.5	L
a_{LH}	14	1/day
a_{FSH}	8.21	1/day
v_{0LH}	212.68	μg/day
v_{1LH}	35,656.90	μg/day
Km_{LH}	170.00	ng/L
$Ki_{LH,P}$	2.81	μg/L
k_{LH}	11.41	1/day
$c_{LH,P}$	0.084	L/μg
$c_{LH,E}$	0.0020	L/ng
d_E	0.50	days
d_P	1.00	days
v_{FSH}	4500.00	μg/day
$Ki_{FSH,InhA}$	646.30	U/L
k_{FSH}	11.55	1/day
$c_{FSH,P}$	3.16	L/μg
$c_{FSH,E}$	0.0023	$(\text{L/ng})^2$
d_{InhA}	1.74	days
α	0.30	dimensionless
β	0.020	dimensionless
γ	0.010	dimensionless
b	0.60	L/day
c_1	1.56	1/day

Param.	**Value**	**Units**
c_2	0.55	$(\text{L}/\mu\text{g})^{\alpha}(1/\text{day})$
c_3	0.051	$(\text{L}/\mu\text{g})^{\beta}(1/\text{day})$
c_4	0.027	$(\text{L}/\mu\text{g})(1/\text{day})$
c_5	0.60	$(\text{L}/\mu\text{g})^{\gamma}(1/\text{day})$
d_1	0.70	1/day
d_2	0.70	1/day
k_1	0.60	1/day
k_2	0.65	1/day
k_3	0.70	1/day
k_4	0.80	1/day
Km_F	115.00	μg/L
p	15.00	dimensionless
e_0	0.00	ng/L
e_1	0.025	1/kL
e_2	0.047	1/kL
e_3	0.060	1/kL
p_0	0.00	μg/L
p_1	0.0047	1/L
p_2	0.00016	1/L
h_0	140.00	U/L
h_1	0.020	$(\text{U/L})/\mu g$
h_2	0.00	$(\text{U/L})/\mu g$
h_3	0.63	$(\text{U/L})/\mu g$
h_4	0.020	$(\text{U/L})/\mu g$

Table 3.5 The five most sensitive parameters ranked in order for model eqs.(3.5)-(3.20) with parameters from Table 3.1. The model output for the second column is E2 peak and for the third column is FSH cycle profile. The five most sensitive parameters are the same for both outputs.

Rank	**E2 Peak**	**FSH Cycle**
1	v_{FSH}	v_{FSH}
2	Km_F	v_{0LH}
3	v_{0LH}	Km_F
4	α	Km_{LH}
5	Km_{LH}	α

CHAPTER

4

STRESS

Of interest in this section is the relationship between the hypothalamic-pituitary-ovarian (HPO) axis and the hypothalamic-pituitary-adrenal (HPA) axis. The introduction of stress to a normal cycling female has been shown to stunt and/or delay the preovulatory LH surge [Bre04; Pie09; Bre06; Wag05]. The introduction of even a regimented exercise routine can alter a normal cycle into a dysfunctional one with reduced LH pulse frequency [Lou89; Sou93]. Various definitions of stress exist creating difficult metrics in which to measure response. Stress can be of a physical, psychological, or immunological nature which have all been shown to reduce the levels of gonadotropins such as LH [Bre06]. To simplify this situation we define "stress" as an alteration in circulating cortisol. This is a reasonable use since altered cortisol is indicative of an active stressor on a system and considered the primary stress hormone in humans [Bre04].

The mechanism by which cortisol affect the menstrual cycle is not entirely understood. Suggestions consist of cortisol acting at the pituitary level reducing sensitivity to GnRH or at the hypothalamic level reducing the frequency or amplitude of pulsatile GnRH secretions. In ovariectomized ewes is has been concluded that LH suppression is due to a decrease in pituitary responsiveness to GnRH [Bre04]. Other studies have discussed the conclusion that cortisol acts directly on the hypothalamus suppressing GnRH secretion [Sak93].

In this study we explore possible parameters within an existing mathematical model of the menstrual cycle which when shifted can elicit behavior analogous to the introduction of cortisol to a normal cycling female. We use a model presented in [Cla03] and data from [Wel99] which we will

describe as the Welt data. In this model the hypothalamus and pituitary are a lumped model coupled with a model of ovarian stages and relative ovarian hormone production. We explore parameter changes in the hypothalamus-pituitary lumped model that we believe cortisol could be affecting and giving rise to abnormal cycles.

4.1 Modeling

To study the effect or stress on the menstrual cycle we study how cortisol would affect certain parameters within the model presented in [Cla03]. This model differs from the core model presented in chapter 1 in that progesterone does not affect the recruited follicle and we are using actual progeterone instead of applied progesterone in the system. The formulation of Eqs (4.1) follows what is outlined in section 2.2 with slight changes in the pituitary-hypothalamus model, and the ovarian model changed to not account for the autocrine effect of progesterone on the recruited follicle. Originally this formulation was presented in [Cla03]. The sub-model given by Eqs (4.1a)-(4.1d) lumps the hypothalamus and pituitary interactions together, so we are not concerned with the effects of cortisol on either of them separately. Generally, we are interested in parameters that modulate the action of the ovarian hormones on the synthesis of LH and FSH. By manipulating these parameters, we indirectly affect the "sensitivity" of the hypothalamus and/or pituitary to the ovarian hormones. We propose that such parameter variations mimic the effect of cortisol either at the level of the hypothalamus via GnRH pulsatility and/or amplitude, or at the level of the pituitary via sensitivity to GnRH.

State Variables

$$\frac{d}{dt}RP_{LH} = \frac{v_{0,LH} + v_{1,LH}\dfrac{(E_2(t-d_e)/Km_{LH})^a}{1+(E_2(t-d_e)/Km_{LH})^a}}{1+\dfrac{P_4(t-d_p)}{Ki_{LH,P}}} - k_{LH}\cdot\frac{1+c_{LH,P}\cdot P_4}{1+c_{LH,E}\cdot E_2}\cdot RP_{LH} \tag{4.1a}$$

$$\frac{d}{dt}LH = \frac{1}{v}\cdot k_{LH}\cdot\frac{1+c_{LH,P}\cdot P_4}{1+c_{LH,E}\cdot E_2}\cdot RP_{LH} - r_{LH}\cdot LH \tag{4.1b}$$

$$\frac{d}{dt}RP_{FSH} = \frac{v_{FSH}}{1+\dfrac{Ih(t-d_{Ih})}{Ki_{FSH,Ih}}} - k_{FSH}\cdot\frac{1+c_{FSH,P}\cdot P_4}{1+c_{FSH,E}\cdot E_2^2}\cdot RP_{FSH} \tag{4.1c}$$

$$\frac{d}{dt}FSH = \frac{1}{v}\cdot k_{FSH}\cdot\frac{1+c_{FSH,P}\cdot P_4}{1+c_{FSH,E}\cdot E_2^2}\cdot RP_{FSH} - a_{FSH}\cdot FSH \tag{4.1d}$$

$$\frac{d}{dt}RcF = b\cdot FSH + (c_1\cdot FSH - c_2\cdot LH^{\alpha})\cdot RcF \tag{4.1e}$$

$$\frac{d}{dt}GrF = c_2\cdot LH^{\alpha}\cdot RcF + (c_3\cdot LH^{\beta} - c_4\cdot LH)\cdot GrF \tag{4.1f}$$

$$\frac{d}{dt}DomF = c_4\cdot LH\cdot GrF - c_5\cdot LH^{\gamma}\cdot DomF \tag{4.1g}$$

$$\frac{d}{dt}OvF1 = c_5\cdot LH^{\gamma}\cdot DomF - d_1\cdot OvF1 \tag{4.1h}$$

$$\frac{d}{dt}OvF2 = d_1\cdot OvF1 - d_2\cdot OvF2 \tag{4.1i}$$

$$\frac{d}{dt}Lut1 = d_2\cdot OvF2 - k_1\cdot Lut1 \tag{4.1j}$$

$$\frac{d}{dt}Lut2 = k_1\cdot Lut1 - k_2\cdot Lut2 \tag{4.1k}$$

$$\frac{d}{dt}Lut3 = k_2\cdot Lut2 - k_3\cdot Lut3 \tag{4.1l}$$

$$\frac{d}{dt}Lut4 = k_3\cdot Lut3 - k_4\cdot Lut4 \tag{4.1m}$$

Auxiliary Equations

$$E_2 = e_0 + e_1\cdot GrF + e_2\cdot DomF + e_3\cdot Lut4 \tag{4.1n}$$

$$P_4 = p1\cdot Lut3 + p2\cdot Lut4 \tag{4.1o}$$

$$Ih = h_0 + h_1\cdot DomF + h_2\cdot Lut2 + h_3\cdot Lut3 \tag{4.1p}$$

The primary hypothalamus and pituitary parameters we test here are Km_{LH}, a, and $v_{1,LH}$. These parameters are found in the equation for LH synthesis Eq (4.1a) and all associated with the

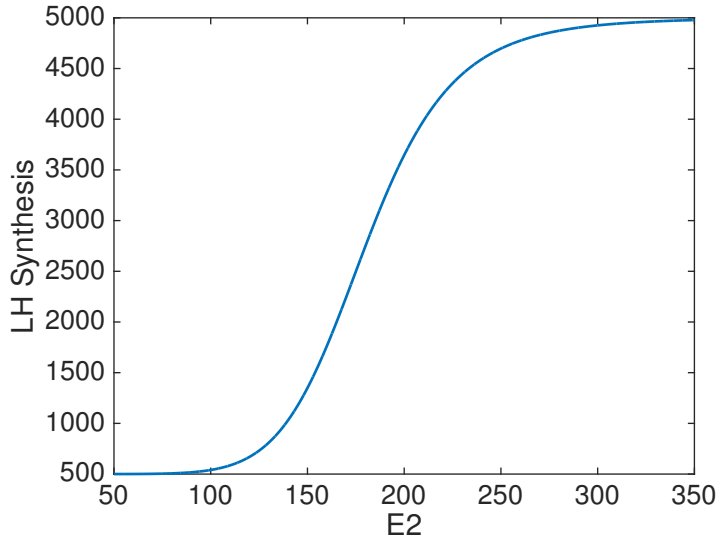

Figure 4.1 Normal LH synthesis. LH synthesis due to E2 levels in the blood under normal conditions using parameters taken from [Har01]. Values represent the amount of LH produced in the reserve pool of the pituitary. The stiff E2 activation of this synthesis is the main mechanism contributing to the LH surge dynamic.

E2 induced LH surge. The LH surge occurs primarily in our model due to a positive feedback of E2 that is represented in the model by a Hill function for LH synthesis. This Hill function is in Eq (4.1a) and is shown separately in Eq (4.2).

$$\mathrm{LH}_{synth} = v_{0,LH} + v_{1,LH}\frac{(E_2(t-d_e)/Km_{LH})^a}{1+(E_2(t-d_e)/Km_{LH})^a} \tag{4.2}$$

Parameter values for our best fit to the Welt data can be found in Table 4.1. The Hill function (Eq (4.2)) representing LH synthesis due to E2 can be seen in Fig 4.1. Any of these values can be altered to change LH synthesis due to E2, and examples of parameter changes to reduce LH synthesis during the LH surge are shown in Fig 4.2. There are qualitative changes in relative LH synthesis due to reduction in either a or $v_{1,LH}$, or an increase in Km_{LH}. Decreasing $v_{1,LH}$ lowers the curve entirely below normal production levels as does the increase in the half max of the Hill function Km_{LH}. The behavior of a however actually raises LH synthesis for low to middle values of E2, but there is decreased synthesis at the higher values of E2 which is critical for inducing a surge.

Parameter values for matching Welt data were taken from [Pas08] and are listed in Table 4.1. Using these values the model generates output matching data shown in Fig 4.3.

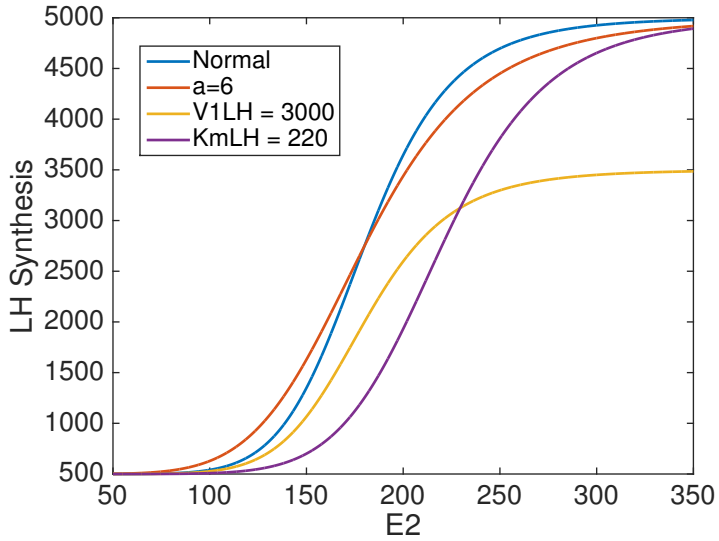

Figure 4.2 Altered LH synthesis. LH synthesis curves under normal conditions, reduced a, reduced $v_{1,LH}$, and increased Km_{LH}. Any of these parameter manipulations are targeted at reducing the LH surge by reducing the effectiveness of E2 to contribute to LH synthesis within the pituitary.

Parameter	Value		Parameter	Value		Parameter	Value
$v_{0,LH}$	500		$c_{FSH,E}$	0.0018		α	0.79
$v_{1,LH}$	4500		d_{Ih}	2.0		β	0.16
Km_{LH}	180		a_{FSH}	8.21		γ	0.02
$Ki_{LH,P}$	12.2		b	0.05		e_0	40
k_{LH}	2.42		c_1	0.09		e_1	0.11
a	8		c_2	0.09		E2	0.21
$c_{LH,P}$	0.26		c_3	0.13		e_3	0.45
$c_{LH,E}$	0.004		c_4	0.027		p_1	0.048
d_E	0.2		c_5	0.51		p_2	0.048
d_P	1.0		d_1	0.50		h_0	0.4
r_{LH}	14		d_2	0.56		h_1	0.009
v	2.5		k_1	0.55		h_2	0.029
v_{FSH}	375		k_2	0.69		h_3	0.018
$Ki_{FSH,Ih}$	3.5		k_3	0.85		$c_{FSH,P}$	12
k_{FSH}	1.90		k_4	0.85			

Table 4.1 Parameter values. Parameter values fitting data from [Wel99]. Model formulation is from [Cla03].

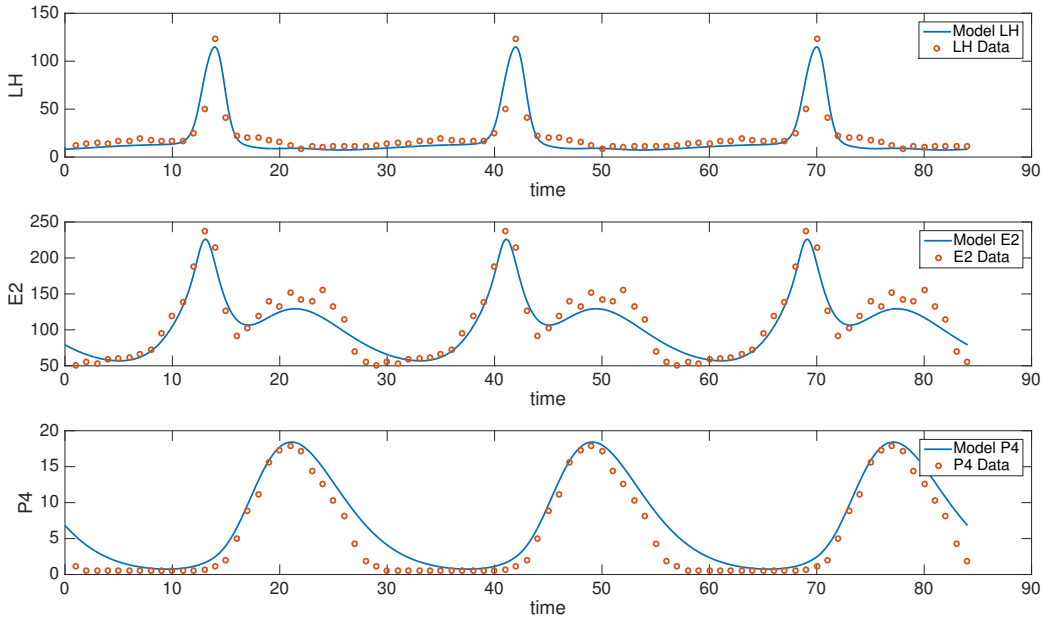

Figure 4.3 Normal cycle. Model simulations (blue curves) of model Eqs (4.1) using parameter values of Table 4.1 are plotted for variables LH, E2, and P4 against the Welt data repeated for 3 cycles. These model solutions have a period of 28 days.

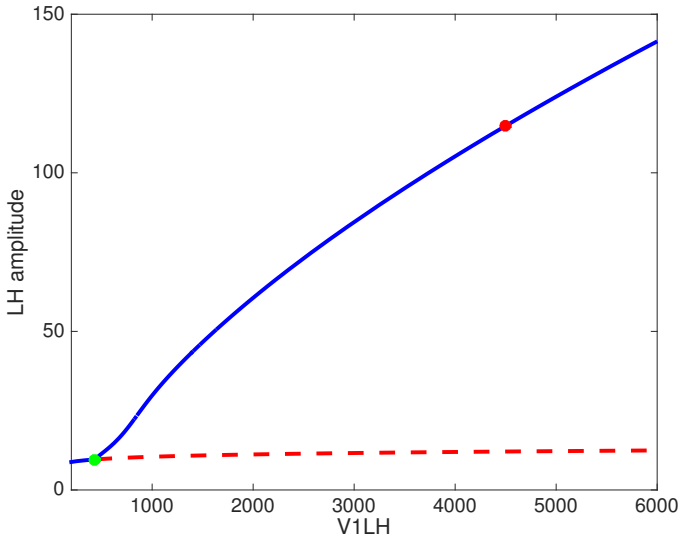

Figure 4.4 Bifurcation for $v_{1,LH}$. Bifurcation diagram for $v_{1,LH}$ with a Hopf bifurcation designated by a green circle and the best fit designated by the red circle. As we decrease $v_{1,LH}$ there is a marked decrease in the amplitude of the LH surge eventually reaching a space of solutions that are period, but lack a high enough LH surge to cause ovulation. Decreasing further ultimately reaching a Hopf bifurcation where the periodic solution disappears and gives way to a stable steady state solution.

4.2 Results

For each of the parameters associated with the Hill function (Km_{LH}, a, and $v_{1,LH}$) we create a bifurcation diagram using the amplitude of the LH surge as a metric. We are most interested in shutting off or stunting this mechanism to produce a non-ovulatory state like induced by physiological stress.

4.2.1 Variation of $v_{1,LH}$

A bifurcation diagram for $v_{1,LH}$ is shown in Fig 4.4. As we decrease $v_{1,LH}$, our LH surge amplitude also decreases becoming anovulatory somewhere near $v_{1,LH} = 2000$ though there is no specific threshold for this distinction. Another effect is an increase in latency to peak and cycle length in general. We calculate the cycle length over the periodic solutions for $v_{1,LH}$ and obtain Fig 4.5. We see that as expected, decreasing $v_{1,LH}$ decreases the LH surge and increases cycle length dramatically once $v_{1,LH}$ falls below the near non-ovulatory values.

4.2.2 Variation of a

The bifurcation diagram for a is shown in Fig 4.6. As we decrease a from the best fit value depicted by a red circle, the amplitude of the LH surge begins to decrease. The parameter a is the exponent in

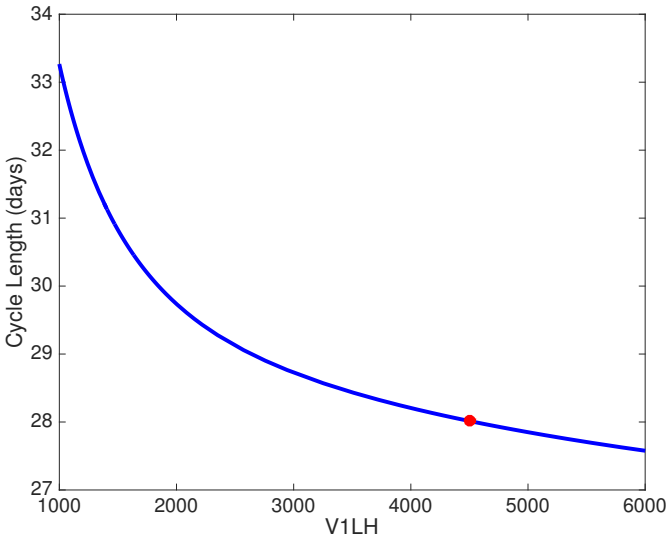

Figure 4.5 Cycle length for $v_{1,LH}$. Cycle Length for $v_{1,LH}$ with the best fit marked by a red circle. As $v_{1,LH}$ is decreased, the cycle length grows longer. All values of $v_{1,LH}$ have reasonable cycle lengths, they become longer at lower values but not outside of physiological reasonability.

our Hill function and controls how E2 contributes to LH synthesis at certain levels. The LH synthesis due to E2 under normal conditions and with a decreased a is shown in Fig 4.2. We see that when a is decreased higher values of E2 do not stimulate as much LH synthesis. This inability of E2 to stimulate LH synthesis at the higher values dampens the surge to non-ovulatory levels as we see in the bifurcation diagram shown in Fig 4.6. Once a is decreased sufficiently the solution passes through a Hopf bifurcation depicted by a green circle. Again we show a plot of cycle length of the period solutions for a depicted in Fig 4.7. The cycle length initially moving from best fit decreased slightly, but then as expected begins to increase rapidly when nearing non-ovulatory values.

4.2.3 Variation of $K\,m_{LH}$

The bifurcation diagram for $K\,m_{LH}$ is shown in Fig 4.8. This parameter determines the location of half maximum synthesis of LH due to E2. Increasing this parameter will shift the curve to the right, meaning that for the same values of E2 we are operating at a lower LH synthesis. A shifted curve and normal curve are depicted in Fig 4.2. When increasing $K\,m_{LH}$ we see a slight decrease in LH surge until the emergence of a saddle node near $K\,m_{LH} = 300$, but not displaying the same magnitude of decrease as either $v_{1,LH}$ or a. There is a second stable periodic solution of very low amplitude around $K\,m_{LH} = 250$. This is of interest possibly suggesting that at these values of $K\,m_{LH}$ a large perturbation in the system could move a person from a near normal cycle to a low amplitude non-ovulatory cycle. The two stables cycles at $K\,m_{LH} = 249$ are depicted in Fig 4.9. Another possible

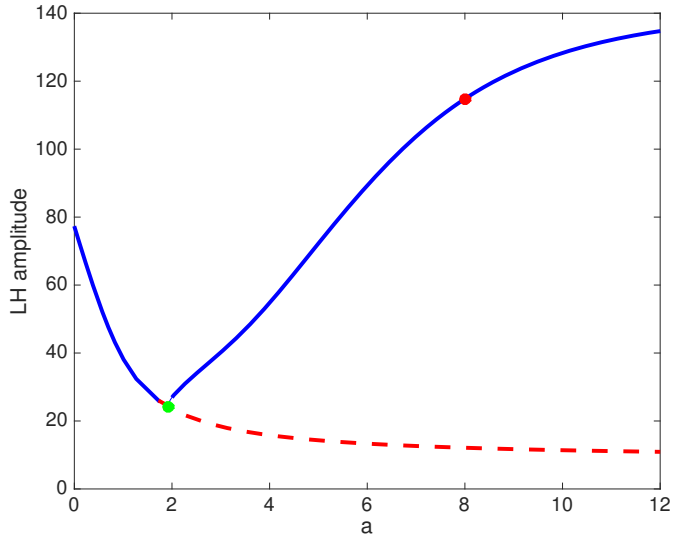

Figure 4.6 Bifurcation for a. Bifurcation diagram for a with a Hopf bifurcation designated by a green circle and the best fit designated by the red circle. As a decreases the amplitude of the LH surge decreases and reaches non-ovulatory values and then passes through a Hopf bifurcation where the periodic solutions changes to a stable steady state.

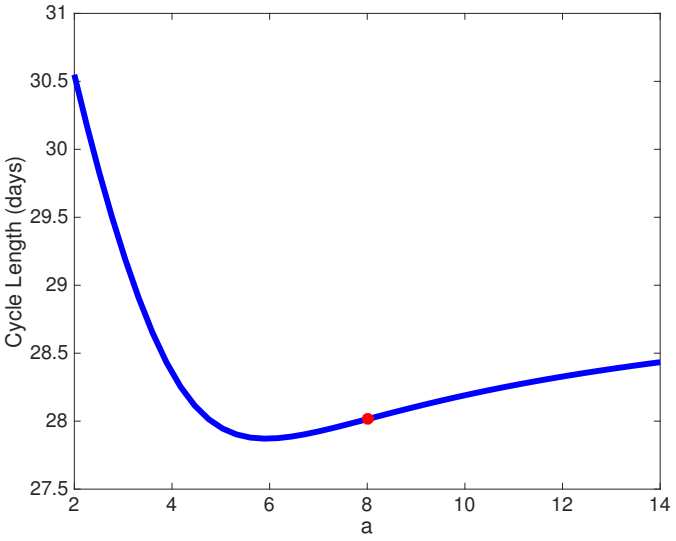

Figure 4.7 Cycle length for a. Cycle Length for a with the best fit marked by a red circle. The range of explored values for a all lead to reasonable cycle times. The primary effect was on the amplitude of the LH surge.

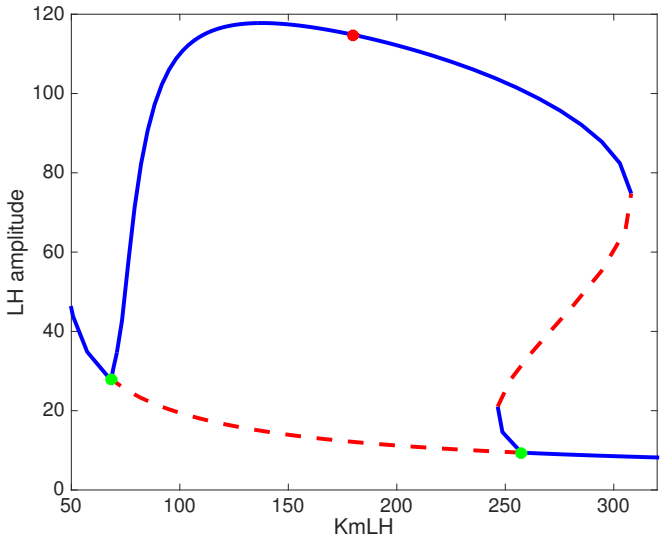

Figure 4.8 Bifurcation for Km_{LH}. Bifurcation diagram for Km_{LH} with Hopf bifurcations designated by a green circle and the best fit designated by the red circle. The two Hopf bifurcations give rise to periodic behavior within a range of values for Km_{LH}. Near the middle of this range is our best fit to our data from [Wel99]. At higher levels of Km_{LH} are two saddle nodes leading to a hysteresis behavior. Note that Km_{LH} has to be raised a fairly significant amount to prevent ovulation. The normal value for Km_{LH} is 226.

behavior is if Km_{LH} were pushed past the saddle node near $Km_{LH} = 300$, reducing it would first default to an abnormal cycle until Km_{LH} was pushed below about 245. This behavior is known as hysteresis and saddle nodes are often associated with this behavior.

4.3 Discussion

Although the model is able to take into account several factors, there is room for improvement. As mentioned above such minor stress as daily exercise can cause a dysfunctional cycle. More research needs to be performed and more data needs to be collected to be able to tie these mechanisms together to the other pathways they are involved in. For instance, in this model we have considered the hypthalumus and pituitary to be lumped. A more specific model incorporating GnRH and the possible effect cortisol has on sensitivity, synthesis, and release may be necessary. Ideally the future model will be more quantitative and react more realistically to changes in concentration, and therefore, input variables. This would require a more solid understanding of the mechanism through which cortisol is acting on the system to reduce LH synthesis and data from women in a stress induced dysfunctional cycle. Moreover it would be benificial to couple the menstrual cycle model to an HPA axis model for example the models by Ottesen *et al.* [Vin11; Ban17; And13].

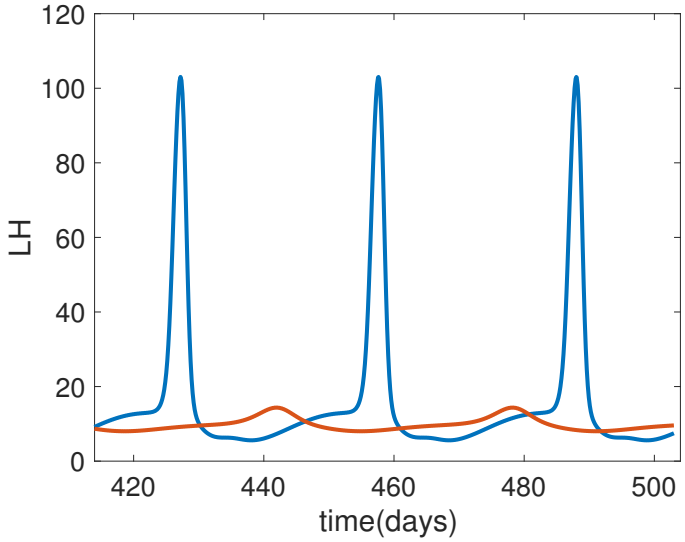

Figure 4.9 Example of bi-stability. Two stable solutions for $Km_{LH} = 249$. This indicates that a large enough change in a natural state can leave in individual on an abnormal cycle despite seemingly normal conditions. This could happen due to a large change in Km_{LH}, mainly increasing it past the saddle node, and then lowering it, past the Hopf bifurcation, but not to the other saddle node. This behavior is known as hysteresis.

CHAPTER

5

CONTRACEPTION

5.1 Note

The paper "Mechanistic model of hormonal contraception" was published open access to PLOS Computational Biology, e1007848 in June 2020. My role in this paper consisted of: model modification from original model in [Mar11], optimization and sensitivity analysis of new model, dynamical analysis of dose response using DDEBifTool, and primary contribution to writing of the paper. Most sections and results are taken verbatim from this paper.

5.2 Introduction

The menstrual cycle involves a complex interaction between the ovaries and the hypothalamus and pituitary in the brain. During the cycle, gonadotropin releasing hormone (GnRH) produced by the hypothalamus and ovarian hormones affect the anterior pituitary. In response the pituitary releases gonadotropins including luteinizing hormone (LH) and follicular stimulating hormone (FSH). These gonadotropins stimulate the ovarian system controlling follicle growth and hormone production. The hormones produced by the follicles, notably estradiol (E2), progesterone (P4), and inhibin A (InhA), feedback onto the brain influencing pituitary hormone production [Fri11].

Hormonal contraception has been in development since the early 20th century with the first FDA approved contraception appearing in 1960 [CM13; Bur11]. Hormonal contraceptives were mainly

composed of synthetic progesterone (a progestin) or a progestin and a synthetic estrogen such as ethinyl estradiol. If these hormones are introduced individually, each can cause contraceptive effects, but high doses of hormonal contraceptives increase the risk for cardiovascular events most notable venous thromboembolism (VTE) and myocardial infarction (MI)[Bur11; Dol76; Man75; Man76; Slo81; Pow75; Ves70; Wil88]. Combined hormonal contraceptives (ethinyl estradiol and progestin together) were discovered during testing of a progestin based contraceptive that was accidentally contaminated with a form of estrogen and shown to increase cycle stability and decrease unwanted bleeding patterns [Che92]. One way to study the effect of administering a combined dose is to use mathematical modeling, which can provide additional insight into effects of varying progestin and synthetic estrogen type and dose.

A number of mathematical models capture dynamics of normal cycling, many of which are based on the formulation by Schlosser and Selgrade [Sel99; Sch00]. These models are on a time scale of days and predict mean levels of hormone [Cla03; Mar11]. To our knowledge there have been no adaptations of mathematical models to predict contraceptive effects of exogenous progesterone and estrogen. Specifically, the original menstrual cycle models by Clark et al. [Cla03] and Margolskee and Selgrade [Mar11] do not include ovarian autocrine effects, and therefore they cannot predict the contraceptive response to exogenous administration of progestins.

The model developed in this study, including ovarian autocrine effects, is used to test hormonal contraceptive treatments via oral administration of ethinyl estradiol and progestin. These treatments are modeled by modifying state variables for blood concentrations of E2 and P4. The model does not include a pharmacodynamic component determining how much or how long it takes for specific amounts of oral contraceptives to produce specific changes in the amount of E2 and P4. Therefore, we administer ethinyl estradiol and progestin as concentrations and assume that contraception is attained if model simulations show a reduction in the LH surge to non-ovulatory levels and/or in P4 levels throughout the cycle.

Model simulations confirm that low and high doses of exogenous progestin reduce the LH surge to non-ovulatory levels as suggested by clinical data [Obr06; Dui18] for progestin treatments. Also low and high doses of exogenous estrogen reduce the LH surge to non-ovulatory levels. And a combination of low dose estrogen and low dose progestin administered together result in constant non-ovulatory hormone levels. The model may be used to predict which dosing levels of estrogen and progestin produce contraceptive cycles. In addition, model simulations indicate how quickly a combined contraceptive treatment produces a non-ovulatory menstrual cycle and how fast the cycle returns to normal after the treatment ends. These simulations were done to motivate clinical experimentation with similar contraceptive combinations.

5.3 History of Contraceptive Development

It is estimated that the average woman would bear 15 children in her reproductive lifetime assuming she is fertile. The expected live births in pre-modern society ranged from 4.5 to 6.5. With high mortality rates on average only two children would survive per couple [Bon83]. It was not until more modern medicine and techniques that the number grew substantially. With the tumultuous nature of child birth in early society however, so called postnatal adjustments of family size acted in place of contraception. Postnatal adjustments include things such as child abandonment, infanticide, adoption, release of young children for apprenticeships and labor [Mas97]. These were not active forms of contraception, but evolved from social necessity of needing to balance out a family that was perhaps to large or small.

Despite birth control not becoming widely acceptable and effective until the 20th century, there have been examples through human history of contraception being experimented with. The earliest depiction is in a cave in France. The painting shows a man engaged in sexual intercourse and using what appears to be a condom [CM13]. The earliest civilization recognized as implementing birth control is the ancient Egyptians [ST05]. Devices called vaginal pessaries or sponges were composed of crocodile dung, honey, and sodium bicarbonate. These could be soaked in acai berry juice that had been fermented. The environment created by the fermented juice was too acidic for sperm to survive [ST05]. Later in history, reference to contraception can be found in Graeco-Roman texts and mediaeval Arabic writings [McL90b]. The first greek writer to discuss contraception was Aristotle and described a method of using olive oil on the womb to prevent pregnancy [CM13]. In addition Greek women were known to use plants such as pomegranates, pennyroyal, and pine as elements in contraceptive techniques [Rus94]. It has been proposed that in classical times herbal contraceptives intended to be taken orally were effective and widely used [Rid97].

It is not until the late 19th century that modern well-known contraceptive techniques were adapted [Coa86]. These did not include hormonal treatments that we know of today, but were more related to the diaphragm and condom. Condoms made from fish or animal gut had been in use in Europe since the 16th century. Initially used to curb the spread of syphilis and then later as a contraceptive device [CM13]. The major change came in 1944 when Charles Goodyear patented the vulcanization of rubber which allowed for mass production of rubber condoms. Until this point in the 20th century contraception was achieved mainly through abstinence, infrequent coitus, coitus interruptus, breastfeeding, and induced abortions [CM13]. Coitus interruptus was responsible for reduction in unintended pregnancies in the UK, but condoms and spermicide became more prominent early in the 20th century [Lan91]. In the United States coitus interruptus was less popular than in the UK with diaphrams and periodic abstinence being used in favor [Fre59]. It was not until the mid to late 20th century that hormonal birth control was discovered and became prominent.

The main name in the development of birth control is American Margaret Sanger. Planned

Parenthood was originally known as The American Birth Control League which Sanger founded. She and her sister opened a birth conrtol clinic in 1916 in Brooklyn which they were arrested for and jailed for 30 days [Cle02]. Ultimately in an appeal she was allowed to keep her clinic open with her being allowed to spread information about illness or disease resulting from pregnancy. She was passionate about change to contraceptive attitudes and poilcy. She once said "No woman can call herself free who does not own and control her body. No woman can call herself free until she can choose consciously whether she will or will not be a mother" [Che92]. This represented the new view forming worldwide about women's personal control over their body. Up until this point the most common contraceptives (coitus interruptus and condoms) were male implemented forms of contraception. With the advent of hormonal contraceptives the power was placed with women instead, giving rise to new attitudes and standards.

Margaret Sanger had two prominent allies during the rise of contraception. The first was Katharine McCormick whom Sanger met through involvement in women's rights. McCormick was married to the inventor of the automatic harvester. In the mid 20th century, McCormick's husband had died leaving a vast fortune that she invested into the development of the first hormonal birth control [Con99].

Sanger and McCormick enlisted the help of reproductive biologist Dr. Gregory Pincus. The goal was a non-mechanical form of contraception for women. McCormick funded a great deal of the project with the total of her contribution exceeding $2 million. The research began with animal trials of progesterone conducted by Pincus. Eventually more potent synthetic progestins were developed for oral use. These synthetic progestins caused unacceptable levels of bleeding. Through a mistake where progestins were contaminated with menstranol, it was discovered that an estrogen component reduces problematic bleeding [CM13]. This lead to the development of a combined hormonal treatment containing both a progestin and an estrogen component.

In 1957 the FDA approved a combined hormonal pill to be used to menstrual disorders. It was two years later before a hormonal pill that would be marketed as a contraceptive was submitted to the FDA. The next year in 1960 the FDA approved the very first hormonal birth control pill [CM13; Bur11]. Around this same time similar hormonal pills were approved in many European countries [Cle02].

The pill became extremely popular amongst contraceptive users. In a ten year period from 1955 to 1965 females using contraceptives began using the pill more prominently. In that decade the portion of non-Hispanic White contraceptors using the pill went from 0 to 24% [Ryd67]. With the rise of the pill the popularity of diaphragms and condoms amongst contraceptors fell. By 1982 the proportion of contraceptors using condoms and diaphragms were 7% and 4% respectively [Pic98]. A similar reaction to the introduction of the pill was happening in the UK. By 1976 38% of married contracepting women were using the pill. The introduction of the pill had a large impact on the fertility of developed countries. In 1950 the expected births per woman was 2.8, and in 2005 it was

1.5 births per woman [Wes76]. Having this number below 2 allows for population stability or even shrinkage.

There were drawbacks to the pill when initially introduced. Some mild adverse effects included breakthrough bleeding, nausea, headaches, and weight gain. This could often lead to discontinued use of the contraceptive. Clinical research performed in the years after the pill was approved also showed troubling results. The pill caused increase risk for cardiovascular events most notable venous thromboembolism (VTE) and myocardial infarction (MI) due to progestin type and estrogen dose [Ves70; Bur11]. Multiple studies report that the risk of MI is increased by a factor or 2 to 4 for women using the pill [Slo81; Man75; Pow75; Man76; Dol76; Wil88].

Even with a low dose estrogen component there is still an increased risk for cardiovascular events specifically VTE, however relative risk of VTE is reduced if estrogen dose is lowered from 100mcg to 50mcg [Blo95; Smi86]. Progestins are in large derived from testosterone and can cause issues in the body through androgenic behavior and other mechanisms. This can cause interactions other than those intended by progesterone. These interactions are associated with a number of adverse events [SW06]. To counter this the dose of progestin given has also substantially decreased by near a factor of 10 for some progestins [Bur11]. In addition a wide variety of progestins have been developed. These differ in androgenic behavior, interaction with progesterone receptor, interaction with estrogen, and other sometimes significant ways.

5.4 Contraceptive Mechanisms

There is not a specific clinical marker of contraception although many indicators can be used: lack of LH surge, a lack of rise in luteal phase progesterone, or incomplete follicle development. Since it is not feasible to determine cycle timing if ovulation does not occur, contraceptive studies measure progesterone daily, and if P4$<$ 5 ng/mL it is assumed that ovulation is suppressed [Obr06], i.e., P4 can be used as a surrogate marker for contraceptive efficacy. Low progesterone levels or the absence of an LH surge indicates that ovulation and luteinization have not occurred or have not occurred properly. In addition to hormonal effects [Obr06; Mul01], there are physical indicators such as increased cervical mucus viscosity, which can prevent sperm mobility leading to a contraceptive state.

Physiologically, progestin can cause a contraceptive state through multiple mechanisms. The primary is prevention of ovulation, but secondary effects such as thickening of cervical mucus also cause a contraceptive state [Dru06; Obr06; Cro02]. According to [Obr06] ovulation prevention occurs if there is not enough estradiol production to stimulate positive feedback mechanisms necessary for the LH surge. The lack of estradiol production is due to poor follicle development from inadequate LH and FSH support. Progestin reduces LH synthesis directly [Fri11] and by limiting follicular sensitivity to FSH in the early follicular phase [Hei95; Obr06]. The original models by Clark

et al. [Cla03] and Margolskee and Selgrade [Mar11] include progesterone's effect on LH synthesis but do not include progesterone's limiting effect on follicle development via sensitivity to FSH. As a result the original models fail to reproduce contraceptive behavior when administration of exogenous progestins. To capture this effect, our new model introduces a growth limiting factor affecting the early follicle development. Similar to progestins, estrogens act through multiple mechanisms. The primary mechanisms are suppression of LH release by the pituitary [Yen05], included in the models [Cla03; Mar11], and bolstering progesterone's contraceptive effect [Sta13; Fri11], which is not accounted for in the original models. In the model presented here, the latter is included by multiplying progesterone, P4, by an increasing function of estrogen, E2.

The major machanism of progestin in a combined hormonal contraceptive treatment is the same, limiting the sensitivity of follicles to gonadotropins. Estrogen serves two purposes: to limit gonadotropin secretion from the pituitary [Gol08; Fri11], which is effective enough to cause a contraceptive state from estrogen only dosing, and to increase progesterone receptor expression, which increases progesterone's effectiveness [Fri11].

In summary, contraception can be achieved either by administering exogenous progestins, estrogen, or a combination of the two. This study uses modeling to illustrate that the combined treatment is advantageous because contraception can be achieved by administrating significantly lower doses of each hormone.

5.5 Hormonal Contraception Data

Model results are compared with data taken from [Mul01; Obr06; Wel99]. Data for a normal menstrual cycle is taken from [Wel99]. Mean daily hormonal values were measured for a group of 23 younger cycling women and 21 older cycling women. Simulations are compared with the data from the younger set. Data for progestin based contraception is from [Obr06], and contains resulting hormone values for three doses of Org 30659, a progestin of interest in the study. The progestin is administered daily for 21 days while also collecting hormonal concentration data. Simulations for our model are compared with data from the highest dose of Org 30659 given to 17 women. From this data, we have: mean maximum P4, mean E2, mean maximum FSH, and mean maximum LH and corresponding standard deviations over the 21 day treatment period. The combined hormonal contraception simulations are compared with data from [Mul01] which tests effectiveness on ovarian function of a vaginal ring, NuvaRing®, containing both a progestin and an estrogen. The study contained two groups: a group switching from an oral combined hormonal treatment to a vaginal ring (group 1) and a group switching from a vaginal ring to an oral combined hormonal treatment (group 2). Model simulations are compared with the median maximum hormonal levels during day 8-14 of treatment for group 1.

5.6 Modeling

Progestin and estrogen act through different pathways and mechanisms to cause a contraceptive state. Progestin acts by limiting follicular sensitivity to FSH and by inhibiting LH synthesis, whereas estrogen inhibits LH release. Two important autocrine effects in the model capture the basic dynamics of both combined hormonal contraceptives and progestin only treatments. The first is contained in Eq (5.4e) via inhibition of FSH at the ovarian level due to P_{app}. The second, described by Eq (5.5c), enhances the effect of P4 in the presence of estrogen.

It should be noted that the model tracks blood concentrations of ovarian hormones, exogenous progestin and estrogen levels.

Therefore contraceptive "doses" always refer to concentrations. To analyze model dynamics for each contraceptive treatment, model simulations must have reached stable behavior (cyclic or steady state) ensuring that effects of initial conditions have dissipated. To achieve this, we administered the contraceptive drugs three months prior to analyzing simulation results.

The new model studied here is based on the model in Margolskee and Selgrade [Mar11], which cannot predict contraceptive behavior. For instance, if a progestin dose of 1.3 ng/mL is administered to the Margolskee and Selgrade model [Mar11], it results in a slightly higher LH surge than the normal. This occurs because a small additional amount of P4 is more effective at increasing FSH production (see Eq (5.4d)) than inhibiting LH production (see Eq (5.4a)). More FSH causes increased early follicular growth (Eq (5.4e) without the P_{app} term) resulting in more early follicular E2 and hence a slightly higher LH surge. Including the P_{app} term without the E2 enhancement of Eq (5.5c) in Eq (5.4a) dampens this growth and decreases the LH surge but it still is at an ovulatory level. Thus in order to model progestin's contraceptive effect both the inhibition of P4 on early follicular development and the enhancement due to E2 are needed to predict contraception.

In the following we describe how the new model components achieve contraception by progestin, estrogen, and the combined treatments.

5.6.1 Progestin Based Contraception

The major mechanism of interest is the inhibiting effect progestin has on FSH's ability to produce follicular tissue that is sensitive to LH. A secondary effect present in Eq (5.4a) is P4's inhibition of LH synthesis. It is believed that the hormonal contraceptive effect of progestin is inhibiting growth of active follicular tissue during the early follicular phase by reducing follicular sensitivity to FSH [Obr06].

This effect is included by introducing P_{app} in Eq (5.4e), which inhibits RcF growth due to FSH. Under normal conditions, the P4 concentration is very low during this part of the cycle, so the inhibitory effect on follicle growth is negligible. Two growth terms proportional to FSH in Eq (5.4e) are divided by a term including the applied progestin. As a result, FSH has less of a stimulatory effect

on follicle growth if the applied progestin is high, such as during treatment with a contraceptive drug or during the luteal phase. These abnormal conditions diminish follicle tissue sensitivity to LH, which inhibits the follicle tissue movement through the normal stages. In addition, the progestin effect is increased by E2 via the Hill function in P_{app} (see Eq (5.5c)). Thus little appreciable follicular mass can reach the growing follicle stage GrF, preventing the mid-cycle rise in E2. Without the rise in E2, the LH surge does not happen and ovulation cannot occur.

5.6.2 Estrogen Based Contraception

Estrogen is contraceptive as well. This comes from inhibiting the release of both LH and FSH from the pituitary, modeled by Eqs. (5.4a) and (5.4c). The end result is the same as with progestin. Insufficient gonadotropins from the pituitary prevent a LH surge. The addition of estrogen to the treatment allows for a smaller dose of progestin.

5.6.3 Combined Hormonal Contraception

In the combined treatment with estrogen and progestin, estrogen serves to bolster progesterone's effect but also inhibits LH release [Fri11]. The presence of estrogen upregulates progesterone receptor expression, which increases P4's effectiveness. This has been shown in ovine and rat uterine cells [Fri11; Tor97]. A possible secondary effect of the the mid-cycle rise in estrogen is to prime P4 receptors for the luteal phase [Tor97]. To represent this dynamic we have added Eq (5.5c), which scales circulating P4 in the body with a steep Hill function dependent on estrogen. The resulting P_{app} is used as the active progesterone in the system. Without estrogen P_{app} is half of the produced P4. At a certain level of estrogen the receptor expression is assumed higher and P_{app} approaches P4. In addition, the Hill function in Eq (5.5c) depends on estrogen causing progestin to be effective at lower doses if there is also an estrogen component.

5.6.4 Model Summary

The model described above is formulated as a system of 13 delay differential equations of the form

$$\frac{dx}{dt} = f(x, y, t, t-\tau), \tag{5.1}$$

where

$$x = \{RP_{LH}, LH, RP_{FSH}(t-\tau), FSH, RcF, GrF, DomF, Sc_1, Sc_2, Lut_1, Lut_2, Lut_3, Lut_4\} \tag{5.2}$$

with four auxiliary equations for the ovarian hormones

$$y = \{E_2, P_4, P_{app}, InhA\} \tag{5.3}$$

and 46 parameters given in Table 1. Estimated parameters are marked in bold and the remaining parameters are from [Mar11]. New parameters are marked by a *.The clearance rate for FSH is from [Cob69]. The clearance rate for LH is from [Koh68]. Equations are solved with MATLAB using the delay differential equation solver (dde23) and bifurcation analysis is done using DDE-BIFTOOL [Eng00].

State Variables

$$\frac{d}{dt}RP_{LH} = \frac{V_{0,LH} + \frac{V_{1,LH}E_2^8}{Km_{LH}^8+E_2^8}}{1+P_{app}/Ki_{LH,P}} - \frac{k_{LH}[1+c_{LH,P}P_{app}]RP_{LH}}{1+c_{LH,E}E_2} \tag{5.4a}$$

$$\frac{d}{dt}LH = \frac{1}{v}\frac{k_{LH}[1+c_{LH,P}P_{app}]RP_{LH}}{1+c_{LH,E}E_2} - a_{LH}LH \tag{5.4b}$$

$$\frac{d}{dt}RP_{FSH} = \frac{V_{FSH}}{1+Inh(t-\tau)/Ki_{FSH,Inh}} - \frac{k_{FSH}[1+c_{FSH,P}P_{app}]RP_{FSH}}{1+c_{FSH,E}E_2} \tag{5.4c}$$

$$\frac{d}{dt}FSH = \frac{1}{v}\frac{k_{FSH}[1+c_{FSH,P}P_{app}]RP_{FSH}}{1+c_{FSH,E}E_2} - a_{FSH}FSH \tag{5.4d}$$

$$\frac{d}{dt}RcF = \frac{bFSH+c_1FSH}{(1+P_{app}/Ki_{RcF,P})^{\xi}}RcF - c_2LH^{\alpha}RcF \tag{5.4e}$$

$$\frac{d}{dt}GrF = c_2LH^{\alpha}RcF - c_3LHGrF \tag{5.4f}$$

$$\frac{d}{dt}DomF = c_3LHGrF - c_4LH^{\gamma}DomF \tag{5.4g}$$

$$\frac{d}{dt}Sc_1 = c_4LH^{\gamma}DomF - d_1Sc_1 \tag{5.4h}$$

$$\frac{d}{dt}Sc_2 = d_1Sc_1 - d_2Sc_2 \tag{5.4i}$$

$$\frac{d}{dt}Lut_1 = d_2Sc_2 - k_1Lut_1 \tag{5.4j}$$

$$\frac{d}{dt}Lut_2 = k_1Lut_1 - k_2Lut_2 \tag{5.4k}$$

$$\frac{d}{dt}Lut_3 = k_2Lut_2 - k_3Lut_3 \tag{5.4l}$$

$$\frac{d}{dt}Lut_4 = k_3Lut_3 - k_4Lut_4 \tag{5.4m}$$

(5.4n)

Auxiliary Equations

$$E_2 = e_0 + e_1 GrF + e_2 DomF + e_3 Lut_4 + e_{dose} \tag{5.5a}$$

$$P_4 = p_0 + p_1 Lut_3 + p_2 Lut_4 + p_{dose} \tag{5.5b}$$

$$P_{app} = P_4 \left(.5 + .5 \frac{E_2^{\mu}}{Km_{P_{eff}}^{\mu} + E_2^{\mu}} \right) \tag{5.5c}$$

$$Inh = h_0 + h_1 DomF + h_2 Lut_2 + h_3 Lut_3 \tag{5.5d}$$

Table 5.1 Parameter values. Parameter values used with model given by Eqs (5.4) and (5.5) for best fit to data from [Wel99].

Hypothalamus/Pituitary			Ovaries					
Name	**Value**	**Unit**	**Name**	**Value**	**Unit**	**Name**	**Value**	**Unit**
$v_{0,LH}$	500	IU/day	$\boldsymbol{b}$	0.34	$\frac{L}{IU} \cdot \frac{\mu g}{day}$	e_0	30	pg/mL
$v_{1,LH}$	4500	IU/day	$Ki_{RcF,P}$*	1	mL/ng	e_1	0.12	L^{-1}
Km_{LH}	175	mL/pg	ξ*	2.2	(none)	e_2	0.32	L^{-1}
$Ki_{LH,P}$	12.2	mL/ng	$\boldsymbol{c_1}$	0.25	$\frac{L}{IU} \cdot \frac{1}{day}$	e_3	0.67	L^{-1}
k_{LH}	2.42	day^{-1}	c_2	0.07	$\left(\frac{L}{IU}\right)^{\alpha} \cdot \frac{1}{day}$	p_0	0.8	ng/mL
$c_{LH,P}$	0.26	mL/ng	c_3	0.027	$\frac{L}{IU} \cdot \frac{1}{day}$	p_1	0.06	kL^{-1}
$c_{LH,E}$	0.004	mL/pg	c_4	0.51	$\left(\frac{L}{IU}\right)^{\gamma} \cdot \frac{1}{day}$	p_2	0.05	kL^{-1}
a_{LH}	14	day^{-1}	d_1	0.5	day^{-1}	$\boldsymbol{Km_{Peff}}$*	75	mL/ng
v_{FSH}	375	IU/day	d_2	0.56	day^{-1}	μ*	8	(none)
τ	1.5	day	k_1	0.69	day^{-1}	h_0	0.4	IU/mL
$Ki_{FSH,Inh}$	1.75	IU/mL	k_2	0.86	day^{-1}	h_1	0.009	IU/(μg·mL)
k_{FSH}	1.9	day^{-1}	k_3	0.85	day^{-1}	h_2	0.029	IU/(μg·mL)
$c_{FSH,P}$	12	mL/ng	k_4	0.85	day^{-1}	h_3	0.018	IU/(μg·mL)
$c_{FSH,E}$	0.0018	mL^2/pg^2	α	0.79	(none)	p_{dose}	0, 0.6, or 1.3	ng/mL
a_{FSH}	8.21	day^{-1}	γ	0.02	(none)	e_{dose}	0, 40, or 92	pg/mL

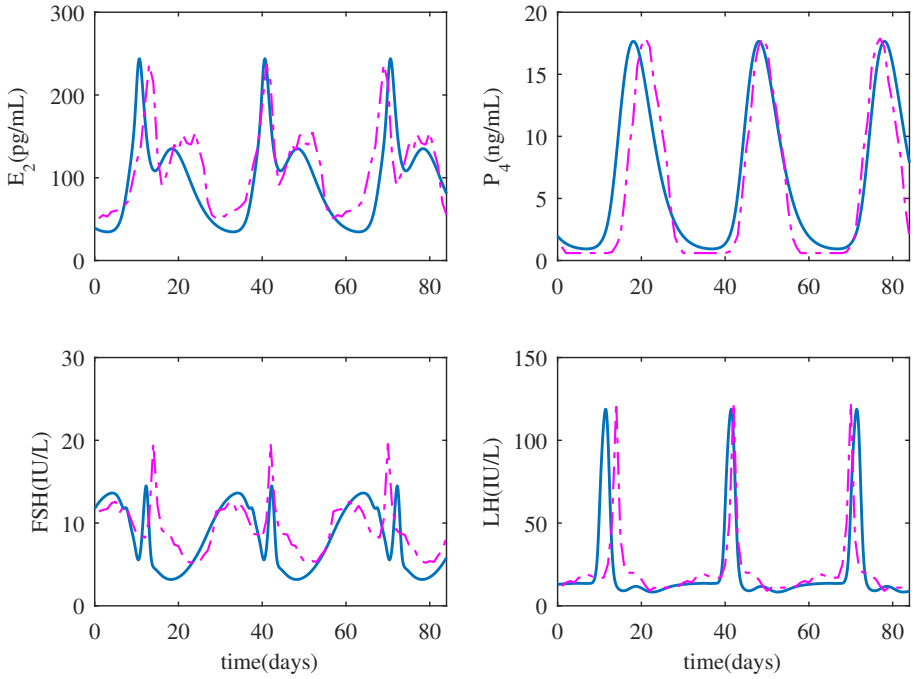

Figure 5.1 Normal cycle. Results for a normal cycle with no exogenous estrogen or progestin. Model output is the solid blue line and the connected points are data taken from [Wel99]

.

5.7 Results

This study presents a mathematical model of the menstrual cycle that functions properly in a normal cycling case and behaves appropriately when dosed with exogenous progestins and estrogens. There are four meaningful cases to consider: a normal contraceptive free cycle, progestin only based contraception, estrogen only based contraception, and combined hormonal contraception. Simulations for a low and high dose for progestin only and estrogen only are presented. The combined hormonal treatment is achieved with two low doses from the single hormone treatments.

Fig 5.1 shows the model's fit to data of normal cycling women taken from [Wel99]. The data is for a single cycle and we have concatenated it for the number of cycles necessary to compare simulations. The model reaching a steady state from contraceptive treatment we define as "total contraception." While biological contraception is achieved before this extreme point, quantitatively it is useful to look at where total contraception takes place for comparative analysis. In all plots unless otherwise stated, asymptotic solutions of a stable cycle or a steady state are displayed. Dosing happens 3 months before time zero and continues throughout the simulations.

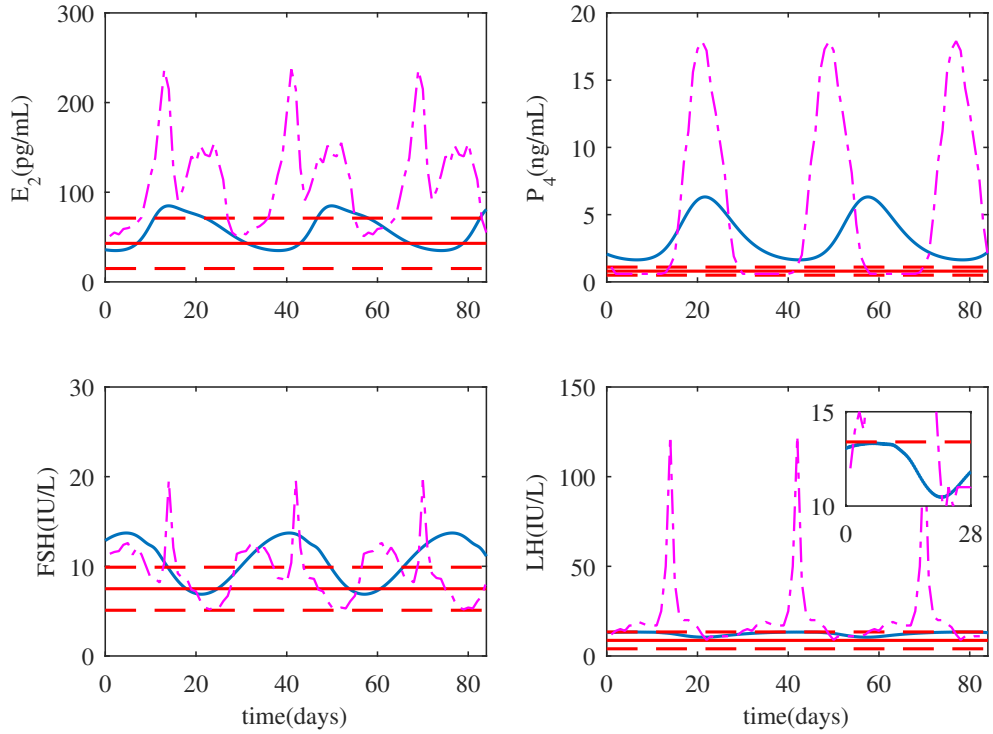

Figure 5.2 Progestin low dose. Model result with low dose ($p_{dose} = 0.6$ng/mL). The solid blue line is the model output. The solid red horizontal line is the mean maximum hormonal value over the 21 day progestin treatment with the standard deviation being represented by the horizontal dotted lines. The mid-cycle LH surge has been eliminated. With this dose we have reached biological contraception by preventing the LH surge, but we have not reached our defined total contraception.

5.7.1 Progestin Based Contraception

With the addition of exogenous progestin, the model approaches a contraceptive state in a dose-dependent manner. Data for a contraceptive state due to progestin is taken from [Obr06]. The data displays the mean maximum and standard deviation of the hormonal values over the 21 day treatment of a progestin based contraceptive. The mean maximum value is denoted with the red solid horizontal line and the standard deviation is represented by the red dotted horizontal line in Fig 5.2 and 5.3. Data from [Wel99] for a normal cycle is plotted for reference in the figures. Results from both a low and a high dose of progestin are shown. The low dose case ($p_{dose} = 0.6$ng/mL) is depicted in Fig 5.2. This dose does not reach total contraception, but the LH surge has been effectively eliminated likely causing biological contraception. In Fig 5.3 the high dose case ($p_{dose} = 1.3$ng/mL) is displayed and steady state has been reached, i.e. our defined total contraception.

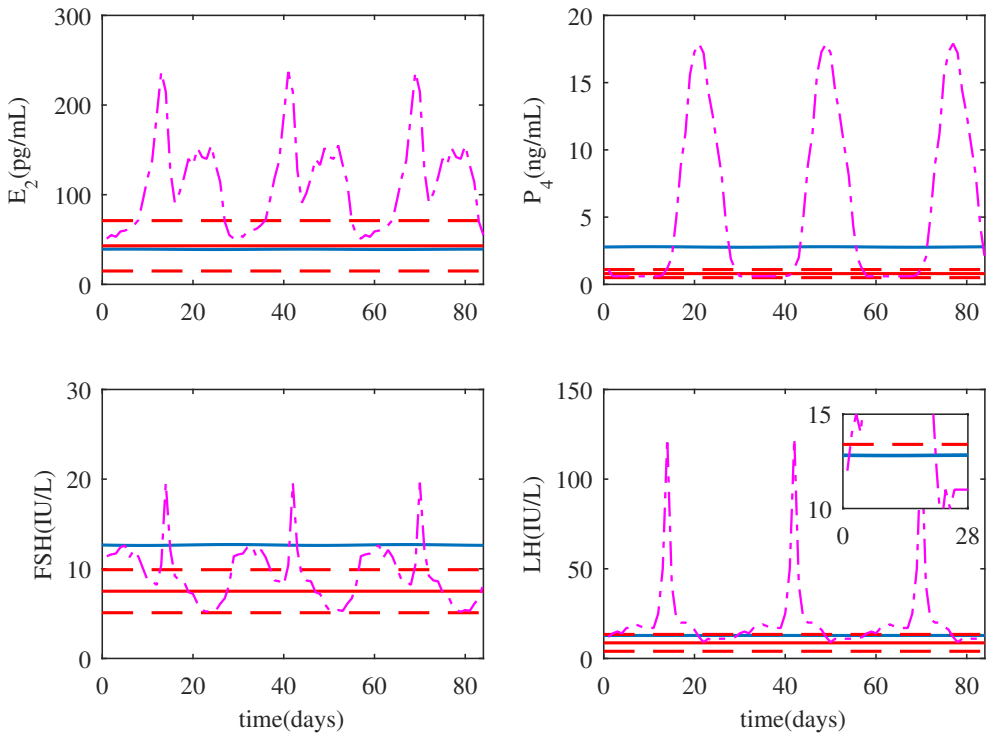

Figure 5.3 Progestin high dose. Model results with high dose $p_{dose} = 1.3$ng/mL. The solid blue line is the model output. The solid red horizontal line is the mean maximum hormonal value over the 21 day progestin treatment with the standard deviation being represented by the horizontal dotted lines. We have reached a steady state here and thus total contraception as we have defined it.

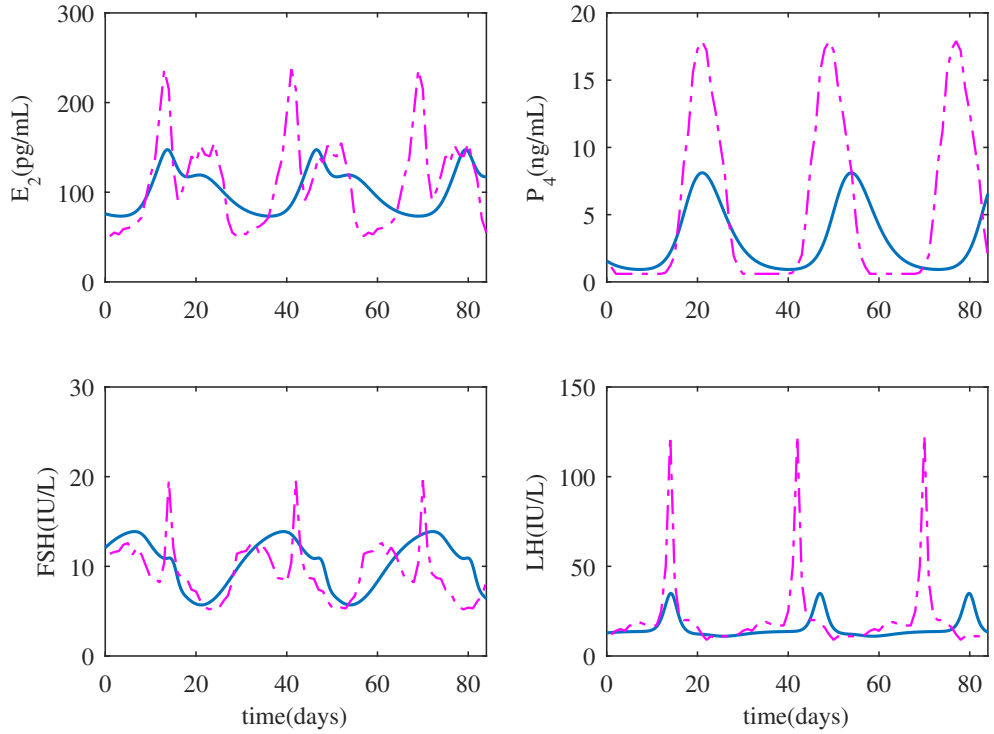

Figure 5.4 Estrogen low dose. Model results with $e_{dose} = 40$pg/mL. The solid blue line is the model output. The LH surge has been mostly eliminated, but hormones still have a large amplitude during the cycle.

5.7.2 Estrogen Based Contraception

While estrogen only contraceptives are not normally used in practice, a high enough dose of estrogen results in contraception. As with progestin, two cases are considered: a low dose that does not cause total contraception and a higher one that does. The low dose case is seen in Fig 5.4. Again, the low dose does not achieve total contraception, but the LH surge has been reduced to a level that would indicate biological contraception. The dose that accomplishes total contraception is seen in Fig 5.5. In both figures, we have plotted data from [Wel99] for reference to a normal cycle. Data for an estrogen only based contraceptive on humans is unavailable, but hormonal values fall within reasonable biological range for a contraceptive state.

5.7.3 Combined Hormonal Contraception

Model hormone predictions are compared with median maximum values taken from [Mul01]. Applying the two low doses to the model at the same time yields the results seen in Fig 5.6. The dotted horizontal line is the median of the max concentration of the hormone between days 8 and 13 of treatment taken from [Mul01]. The solid horizontal line is the predicted hormone concentration output from the model.

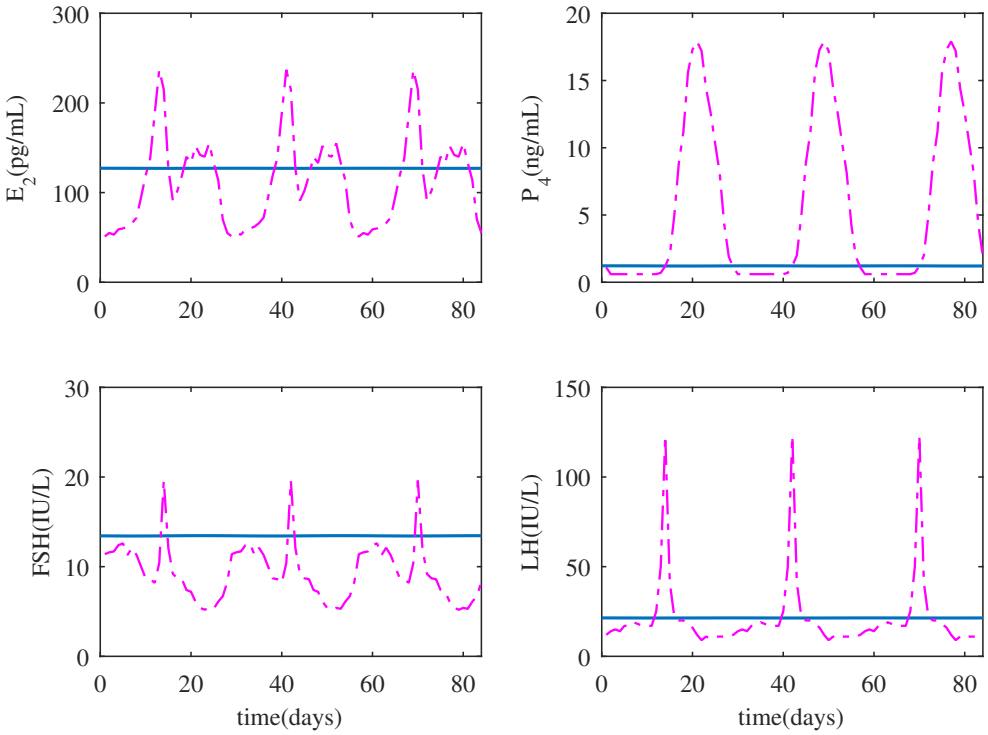

Figure 5.5 Estrogen high dose. Model results with $e_{dose} = 92$pg/mL. The solid blue line is the model output. For this high of a dose a state of total contraception has been reached.

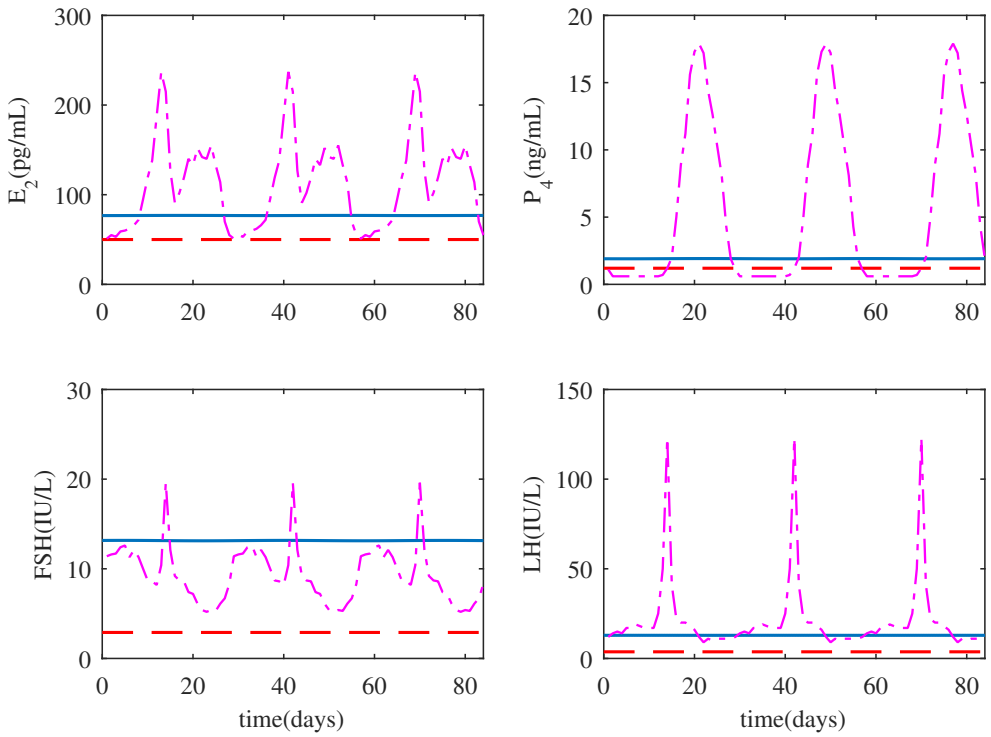

Figure 5.6 Combined low dose. Model results with $p_{dose} = 0.6$ng/mL and $e_{dose} = 40$pg/mL. The solid blue line is the model output. The dotted red line is the median maximum hormonal value during days 8-14 of combined hormonal treatment. These are the two low doses that did not reach total contraception when used individually. The application of both low doses though has achieved total contraception.

5.7.4 Bifurcation Analysis

A bifurcation is a change in qualitative behavior of a system and occurs as a parameter of the system crosses a critical value. A Hopf bifurcation occurs when moving over this critical value causes a change from cyclic behavior to steady state behavior or vice versa. If the model is in a cyclic state a significant enough increase in p_{dose}, e_{dose}, or both will move the model over a Hopf bifurcation from the cyclic region into steady state region. The curve in the (e_{dose}, p_{dose}) space of Hopf bifurcations then illustrates where total contraception is achieved.

A bifurcation curve shown in Fig 5.7 disaplys Hopf bifurcations in the (e_{dose}, p_{dose}) space illustrating the relationship between doses and total contraception. Below the curve are periodic solutions to the model and above the curve are steady state solutions. The normal state of the model is at $(0,0)$ where there is no dose of either type. The Hopf bifurcations define the doses at which total contraception takes place: the exact point at which the periodic solution becomes a steady state solution. The high dose cases for estrogen and progestin are shown as stars on the x and y axis respectively. The combination low dose is marked just above the Hopf curve in the steady state solution space in red. The two high dose treatments can be found along either axis where the Hopf curve intersects: for progestin only at $p_{dose} \approx 1.3$ng/mL and for estrogen only at $e_{dose} \approx 92$pg/mL.

5.7.5 Return to Normal Cycling

All results presented up to this point have been asymptotic solutions that have allowed time for the model to reach a stable cycle or steady state solution. It is imperative, however, in contraceptive design that introduction of a contraceptive quickly cause a non-ovulatory state and removal of the contraceptive results in return to normal cycling. To demonstrate this behavior the model simulates the time for nine cycles to take place assuming cycles are 28 days. The first 3 cycles are normal, the next 3 cycles have a combined low dose of estrogen and progestin, and the last 3 cycles have the dose in the blood exponentially decay due to the drug's half-life. Both half-lives of the drugs are short compared to the model time scale: the progestin has a half-life of a day and estrogen has a half-life of two days. The resulting simulation is shown in Fig 5.8. The vertical dotted lines represent the beginning and end of dosing. The simulation transitions from a normal cycling state to a contraceptive state and back to normal cycling within one to two cycles of the treatment's removal. The contraceptive portion of the simulation does not have time to reach a steady state, but is completely devoid of an LH surge. The combined dose given is strong enough to cause total contraception if treatment was applied for a longer window.

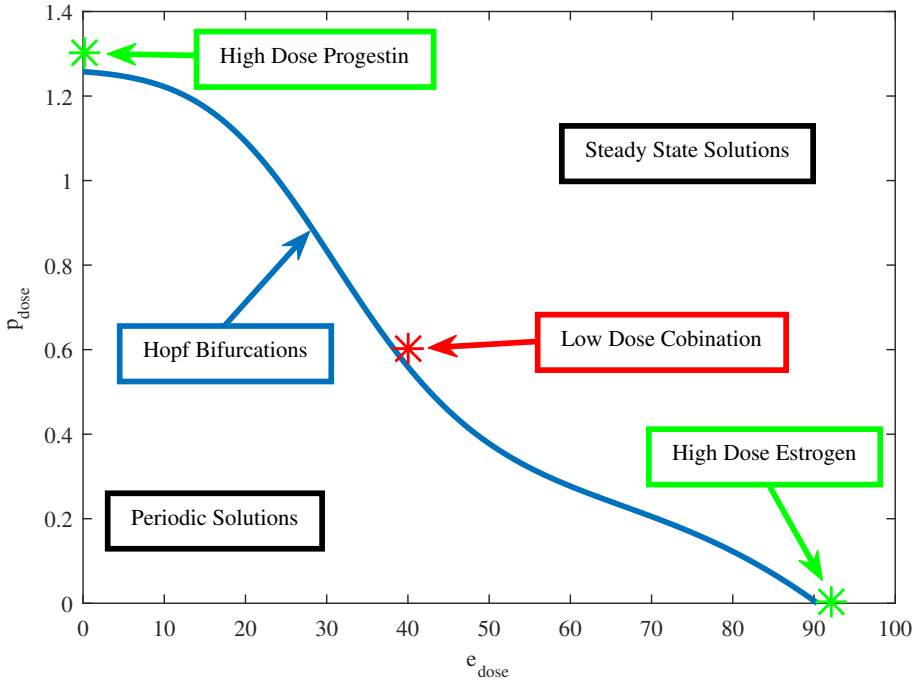

Figure 5.7 Hopf bifurcations. Bifurcation diagram representing location of Hopf bifurcations in the (e_{dose}, p_{dose}) space. Solutions below the curve of Hopf bifurcations are periodic and solutions above the curve are steady state. Our total contraception as we have defined it then occurs along this curve of Hopf bifurcations. Any doses falling above the line are totally contraceptive and any below are not. The low dose combination that we tested is shown with a star and falls just into the steady state region. The progestin and estrogen only doses can be seen by where the Hopf curve intersects the axes.

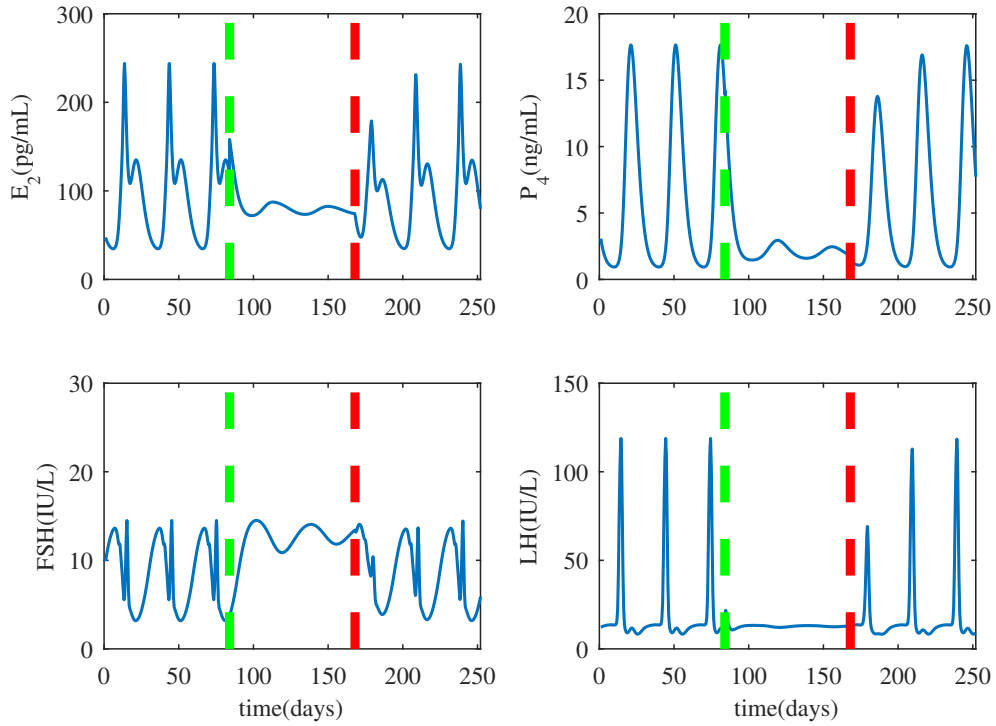

Figure 5.8 Temporary dose. Simulation of a temporary treatment of a low dose combined hormonal contraceptive. Dosing begin at day 84 and ends at day 168 at which point the dose decreases exponentially due to the half-life of the drug. A nearly instant contraceptive effect after dosing is observed and once the drug is removed, return to ovulation occurs within 1-2 cycles.

5.8 Discussion

In this study, we present a system of 13 nonlinear differential equations which models the menstrual cycle dynamics and basic effects of several contraceptive hormone treatments. The model from [Mar11] was modified to include two ovarian autocrine effects: progesterone inhibiting growth of the recruited follicle and estrogen amplifying the effects of progesterone shown in Eq (5.4e) and Eq 5.5c respectively. Data from the biological literature [Wel99] are used to identify model parameters and the resulting model simulations approximate well the hormonal profiles of normally cycling women (Fig 5.1).

Then the model is used to test the effects of five different hormonal contraceptive treatments. It is assumed that the doses of exogenous hormones are added directly to the blood and act as the natural analogues in the body. Low and high doses of exogenous progestin reduce the LH surge to non-ovulatory levels (Fig 5.2 and Fig 5.3) and reflect clinical data [Obr06] for progestin treatments. In fact, the high dose progestin results in total contraception, which means that hormonal levels are at steady-state because the solutions to the differential equations are constants. Also, low and high doses of exogenous estrogen reduce the LH surge to non-ovulatory levels (Fig 5.4 and 5.5). The high dose estrogen causes steady-state hormone levels. When low dose estrogen and low dose progestin are administered together, this combined hormonal treatment achieves total contraception (Fig 5.6) compared with clinical data from [Mul01].

In order to determine which dosing pairs result in total contraception, a Hopf bifurcation curve (Fig 5.7) is drawn in the (e_{dose}, p_{dose}) plane which separates the plane into a region of steady-state solutions and a region of nonconstant periodic solutions. For dosing pairs near this curve, LH and P4 levels are low so the menstrual cycles are non-ovulatory. As both dosing amounts decrease, the LH surge increases and the contraceptive effect is gradually lost. If a non-ovulatory LH level is assumed, the model may be used to predict which dosing pairs result in contraceptive cycles. Results presented here showed that there can be a minimum dose. This can be further reduced with optimal control to determine when dosing should be done. This work can be seen in the [Gav22].

Also, model simulations indicate how quickly a combined contraceptive treatment produces a non-ovulatory menstrual cycle and how fast the cycle returns to normal after the treatment ends. For example, Fig 5.8 shows that the treatment pair $(e_{dose}, p_{dose}) = (40$ pg/mL, 0.6 ng/mL) results in a contraceptive state in the first cycle after dose application and an ovulatory cycle returns within one or two cycles after the treatment ends.

A deficiency of the current model is the predicted FSH response to hormonal treatment. Eq 5.4c indicates that FSH synthesis only depends on Inhibin A. When a contraceptive state is reached, luteinization does not occur and so Inhibin A is diminished. Because Inhibin A inhibits FSH synthesis, the model predicts that in a contraceptive state FSH is produced at a high level. However, this is not observed biologically [Mul01]. To improve the model, Eq 5.4c needs to be modified so that FSH

synthesis depends on more reproductive hormones.

Finally, for each synthetic exogenous hormone, the addition of a model accounting for its pharmacokinetics and its specific activity in relation to the corresponding natural hormone would allow for more detailed representation of different treatments. Further adaptation of the model combined with sufficient data could provide a useful tool for pre-clinical trial phases.

CHAPTER

6

DISCUSSION

In this dissertation I have presented an overview of current mechanistic modeling of the menstrual cycle and three realizations of this structure applied to different situations. The first model presented is a model of follicle waves taken from [Pan16], a phenomenon where a second large wave of FSH can lead to additional primary follicles being recruited. The model can exhibit menstrual cycles with two or three follicle waves corresponding to the numbers of rises in the cycle of FSH. The inclusion of an atresia term in this model prevents more than one ovulation per cycle. In the abscence of this term it is possible for a second ovulation to occur in a cycle resulting in dizygotic twins via superfecundation. Dynamical analysis of the atresia term shows a cascade of period doubling bifurcations resulting in possibly chaotic cycles. The beginning of the period doubling cascade is shown in Fig 3.16. The presence of this atresia term changes the dynamical behavior in the model and could produce erratic menstrual cycle behavior.

The second model presented is taken from [Cla03]. Of interest in the analysis was the effect of various parameters related to LH synthesis on the behavior of the cycle. It is believed the primary stress hormone cortisol may act at the level of the hypothalamus or the pituitary affecting sensitivity to ovarian drugs or GnRH or secretion of GnRH. Three parameters were analyzed that could be related to cortisol's affect on synthesis of LH. These parameters are all associated with the Hill function in the LH synthesis term responsible for the LH surge. The first parameter discussed $v_{1,LH}$ does not produce very interesting results. This parameter is the scale of the Hill function and as it decreases so does the synthesis due to E2. The second parameter discussed a is the exponent of

this Hill function. Reducing this value will decrease the amplitude of the LH surge but increases values when E2 is below the half max Km_{LH}. The half max of the Hill function Km_{LH} is the last parameter discussed. In the bifurcation diagram shown in Fig 4.8 we see that raising Km_{LH} from our best fit will reach a saddle node and fall to a steady state solution. A second saddle node results in hysteresis behavior and we have two stable cycles: one ovulatory and one anovulatory. This analysis shows possible places cortisol may be affecting a healthy menstrual cycle. More behavior data of these hormones during a cycle affected by stress is necessary for further study into which of these parameters are relevant in capturing that behavior. In addition the model may need to incorporate other important interactions by including GnRH models or receptor sensitivity to some of the hormones. Further analysis to the model can be done as shown in [Gav22] in which an optimal control scheme is used in order to limit doses further by timing the introduction of the dose.

The last model presented is a model exhibiting cyclic behavior under dosing of hormonal contraceptives: progestin based, estrogen based, and combined treatment. A model from [Mar11] was modified with the addition of two autocrine effects within the ovaries that are important in capturing dynamics of a contraceptive state. Progesterone inhibits through two effects in the mode: progesterone inhibits the growth of the recruited follicle and is more effective in the presence of estrogen. Five cases were shown of hormonal contraceptive dosing: a low and high dose of progesterone, a low and high dose of estrogen, and a combined low dose of both. A simulation shown in Fig 5.8 demonstrates the model's ability to be dosed, reach a contraceptive state, and return to normal cycling after the dose is removed. Results for a dose reaction are show in Fig 5.7. In the figure the high dose of estrogen and progestin are show, and a low dose combination is show in the same anovulatory space. The curve of Hopf bifurcations represent where "total contraception" has occured. The model supports that lower doses can be used in a combined treatment to achieve contraception. Further work in the model will require structural considerations such as the synthesis term for FSH needs to be changed to have FSH synthesis dependent on something not present during a contraceptive state. More comparison to data and the inclusion of some pharmakokenetic would need to be considered to apply specific contraceptive drugs as the model currently considers the contraceptive drugs the same as endogenous cycling hormones.

BIBLIOGRAPHY

[And13] Andersen, M. et al. "Mathematical modeling of the hypothalamic–pituitary–adrenal gland (HPA) axis, including hippocampal mechanisms". *Math BioSci* **246** (2013), pp. 122–138.

[Bae03a] Baerwald, A. et al. "A new model for ovarian follicular development during the human menstrual cycle". *Fertil. and Steril.* **80** (2003), pp. 116–122.

[Bae03b] Baerwald, A. et al. "Characterization of ovarian follicular wave dynamics in women". *Biol. of Reproduction* **69** (2003), pp. 1023–1031.

[Bae12] Baerwald, A. et al. "Ovarian antral folliculogenesis during the human menstrual cycle: a review". *Hum. Reprod. Update* **18** (2012), pp. 73–91.

[Ban17] Bangsgaard, E. & Ottesen, J. "Patient specific modeling of the HPA axis related to clinical diagnosis of depression". *Math Biosci* **287** (2017), pp. 24–35.

[Blo95] Bloemenkamp, K. et al. "Enhancement by factor V Leiden mutation of risk of deep-vein thrombosis associated with oral contraceptives containing a third-generation progestagen". *Lancet* **346** (1995), pp. 1593–1596.

[Bog72a] Bogumil, R. et al. "Mathematical studies of the human menstrual cycle". *J. Clin. Endocr.* **35** (1972), pp. 126–143.

[Bog72b] Bogumil, R. et al. "Mathematical studies of the human menstrual cycle. II: Simulation performance of a model of the human menstrual cycle". *J. Clin. Endocr.* **35** (1972), pp. 144–156.

[Bon83] Bongaarts, J. & Potter, R. G. *Fertility, biology, and behavior*. New York: Academic Press, 1983.

[Bor99] Bortolus, R. et al. "The epidemiology of multiple births". *Hum. Reprod. Update* **5** (1999), pp. 179–187.

[Bre04] Breen, K. & Karsch, F. "Does Cortisol Inhibit Pulsatile Luteinizing Hormone Secretion at the Hypothalamic or Pituitary Level". *J. Endocrinol* **142** (2004), pp. 692–698.

[Bre06] Breen, K. & Karsch, F. "New Insights Regarding Glucocorticoids, Stress, and Gonadotropin Suppression". *Front. Neroendocrinol* **27** (2006), pp. 233–245.

[Bur11] Burkmana, R. et al. "The evolution of combined oral contraception: improving the risk-to-benefit ratio". *Contraception* **84** (2011), pp. 19–34.

[Cha78] Chang, R. & Jaffe, R. "Progesterone effects on gonadotropin release in women pretreated with estradiol". *J. Clin. Endocrinol. Metab.* **47** (1978), pp. 119–125.

[Che14] Chen, C. & Ward, J. "A mathematical model for the human menstrual cycle". *Math. Medicine and Biol.* **31** (2014), pp. 65–86.

[Che92] Chesler, E. *Woman Of Valor : Margaret Sanger and the Birth Control Movement in America*. New York :Simon & Schuster, 1992.

[CM13] Christin-Maitre, S. "History of oral contraceptive drugs and their use worldwide". *Best Pract. Res. Clin. Endocrinol. Metab.* **27** (2013), pp. 3–12.

[Cla03] Clark, L. et al. "Multiple Stable Periodic Solutions in a Model for Hormonal Control of the Mentrual Cycle". *Bull. Math. Biol.* **65** (2003), pp. 157–173.

[Cle02] Cleland, J. "Contraception in historical and global perspective". *Best Pract. Res. Clin. Obstet. Gynaecol.* **23** (2002), pp. 165–176.

[Coa86] "The decline of fertility in Europe". Ed. by Coale, A. J. & Watkins, S. C. Princeton, N.J. : Princeton University Press, 1986.

[Cob69] Coble, Y. et al. "Production rates and metabolic clearance rates of human follicle-stimulating hormone in premenopausal and postmenopausal women". *J Clin Investig.* **48** (1969), pp. 359–363.

[Con99] Connell, E. B. "Contraception in the prepill era". *Contraception* **59** (1999), 7S–10S.

[Cro02] Croxatto, H. "Mechanisms that explain the contraceptive action of progestin implants for women". *Contraception* **4** (2002), pp. 21–27.

[Dev92] Devaney, R. *A First Course in Chaotic Dynamical Systems: Theory and Experiment*. Boca Raton FL: Taylor & Francis Group LLC, 1992.

[Dol76] Doll, R. et al. "Myocardial infarction in young women with special reference to oral contraceptive practice". *BMJ* **2** (1976), pp. 241–245.

[Dru06] Drummond, A. "The role of steriods in follicular growth". *Reprod. Biol. Endocrinol.* **4** (2006), pp. 1–11.

[Dui18] Duijkers, I. et al. "Phase II dose-finding study on ovulation inhibition and cycle control associated with the use of contraceptive vaginal rings containing 17β-estradiol and the progestagens etonogestrel or nomegestrol acetate compared to NuvaRing." *Eur. J. Ctracep. Repr.* **23** (2018), pp. 245–254.

[Eng00] Engelborghs, K. et al. "Numerical bifurcation analysis of delay differential equations". *Jour. of Comput. and Appl. Math.* **125** (2000), pp. 265–275.

[For94] Fortune, J. "Ovarian follicular growth and development in mammals". *Biol. Reprod.* **50** (1994), pp. 225–232.

[Fra89] Franchimont, P. et al. "Inhibin and Related Peptides: Mechanisms of Action and Regulation of Secretion". *J. Steroid Biochem.* **32** (1989), pp. 193–197.

[Fre59] Freedman, R. *Family planning, sterility and population growth*. The study was conducted jointly by the Scripps Foundation for Research in Population Problems, Miami University, and the Survey Research Center, University of Michigan. New York, McGraw-Hill, 1959.

[Fri11] Fritz, M. & Speroff, L. *Clinical Gynecologic Endocrinology and Infertility*. Lippincott Williams and Wilkins, 2011.

[Gav22] Gavina, B. et al. "Toward an optimal contraception dosing strategy". *BioRxiv* (2022).

[Gin05] Ginther, O. et al. "Systemic concentrations of hormones during the development of follicular waves in mares and women: a comparative study". *Reproduction* **130** (2005), pp. 379–388.

[Gol08] Goldzieher, J. & Stanczyk, F. "Oral contraceptives and individual variability of circulating levels of ethinyl estradiol and progestins". *Contraception* **78** (2008), pp. 4–9.

[Hal03] Hall, J. "Twinning". *Lancet* **362** (2003), pp. 735–743.

[Har01] Harris, L. "Differential equation models for the hormonal regulation of the menstrual cycle". PhD thesis. North Carolina State University, 2001.

[HC03] Harris-Clark, L. et al. "Multiple stable periodic solutions in a model for hormonal control of the menstrual cycle". *Bull. Math. Biology* **65** (2003), pp. 157–173.

[Hei95] Heikinheimo, O. et al. "Inhibition of Ovulation by Progestin Analogs (Agonists vs Antagonists): Preliminary Evidence for Different Sites and Mechanisms of Actions". *Contraception* **53** (1995), pp. 55–64.

[Hot94] Hotchkiss, J. & Knobil, E. "The menstrual cycle and its neuroendocrine control". *The Physiology of Reproduction, Second Edition* (1994), pp. 711–750.

[Jam80] James, W. "Gestational age in twins". *Arch. Dis. Childh.* **55** (1980), pp. 281–284.

[Kar73] Karsch, F. et al. "Positive and negative feedback control by estrogen of luteinizing hormone secretion in the rhesus monkey". *J. Endocrinol* **92** (1973), pp. 799–804.

[Kee09] Keener, J. & Sneyd, J. *Mathematical Physiology*. Vol. 1. 8. Springer-Verlag New York, 2009.

[Koh68] Kohler, P. et al. "Metabolic clearance and production rates of human luteinizing hormone in pre- and postmenopausal women". *J. Clin. Invest.* **47** (1968), pp. 38–47.

[LP92] L. Plouffe, J. & Luxenberg, S. "Biological modeling on a microcomputer using standard spreadsheet and equation solver programs: The hypothalamic-pituitary-ovarian axis as an example". *Comput. Biomed. Res.* **25** (1992), pp. 117–130.

[Lan91] Langford, C. M. "Birth Control Practice in Great Britain: A Review of the Evidence from Cross-Sectional Surveys". *Popul. Stud.* **45** (1991), pp. 49–68.

[Liu83] Liu, J. & Yen, S. “Induction of midcycle gonadotropin surge by ovarian steroids in women: A critical evaluation”. *J. Clin. Endocrinol. Metab.* **57** (1983), pp. 797–802.

[Lou89] Loucks, A. et al. “Alterations in the hypothalamic-pituitary-ovarian and the hypothalamic-pituitary-adrenal axes in athletic women”. *J. Clin. Endocrinol. Metab.* **68** (1989), pp. 402–411.

[Man75] Mann, J. I. & Inman, W. H. W. “Oral contraceptives and death from myocardial infarction”. *BMJ* **2** (1975), pp. 245–248.

[Man76] Mann, J. I. et al. “Oral Contraceptive Use In Older Women And Fatal Myocardial Infarction”. *BMJ* **2** (1976), pp. 445–447.

[Mar13] Margolskee, A. “A Whole Life Model of the Human Menstrual Cycle”. PhD thesis. North Carolina State University, 2013.

[Mar11] Margolskee, A. & Selgrade, J. “Dynamics and bifurcation of a model for hormonal control of the menstrual cycle with inhibin delay”. *Math. Biosci.* **234** (2011), pp. 95–107.

[Mas97] Mason, K. O. “Explaining Fertility Transitions”. *Demography* **34** (1997), pp. 443–454.

[McL90a] McLachlan, R. et al. “Serum inhibin levels during the periovulatory interval in normal women: relationships with sex steroid and gonadotrophin levels.” *Clin. Endocrinol.* **32** (1990), pp. 39–48.

[McL90b] McLaren, A. *A history of contraception from antiquity to present day*. Oxford: Blackwell, 1990.

[Mue15] Mueller, B. “Paternity case for a New Jersey mother of twins bears unexpected results: Two fathers”. *New York Times* (2015).

[Mul01] Mulders, T. M. & Dieben, T. O. “Use of the novel combined contraceptive vaginal ring NuvaRing for ovulation inhibition”. *Fertil. Steril.* **75** (2001), pp. 865–870.

[Nel65] Nelder, J. & Mead, R. “A simplex method for function minimization”. *Comput. J.* **7** (1965), pp. 308–313.

[Obr06] Obruca, A. et al. “Ovarian function during and after treatment with the new progestagen Org 30659”. *Fertil. Steril.* (2006), pp. 108–115.

[Ode79] Odell, W. *The reproductive system in women*. Ed. by DeGroot, L. Grune & Stratton, New York, 1979.

[Oje92] Ojeda, S. *Female reproductive function*. Ed. by Griffin, J. & Ojeda, S. Oxford: Oxford University Press, 1992.

[Pan01] Panza, N. “Modeling Follicle Wave Dynamics in the Menstrual Cycle”. PhD thesis. North Carolina State University, 20015.

[Pan16] Panza, N. et al. “A delay differential equation model of follicle waves in women”. *J. Biol. Dyn.* **10** (2016), pp. 200–221.

[Pas08] Pasteur, R. D. “A Multiple-Inhibin Model of the Human Menstrual Cycle”. PhD thesis. North Carolina State University, 2008.

[Pas11] Pasteur, R. & Selgrade, J. *Understanding the Dynamics of Biological Systems: Lessons Learned from Integrative Systems Biology*. United Kingdom: Springer New York, 2011. Chap. 3.

[Pic98] Piccinino, L. J. & Mosher, W. D. “Trends in Contraceptive Use in the United States: 1982-1995”. *Int. Fam. Plan. Perspect.* **30** (1998), pp. 4–46.

[Pie09] Pierce, B. et al. “Cortisol Disrupts the Ability of Estradiol-17β to Induce the LH Surge in Ovariectomized Ewes”. *Domest. Anim. Endocrinol.* **36** (2009), pp. 202–208.

[Pop09] Pope, S. et al. “Estimation and identification of parameters in a lumped cerebrovascular model”. *Math. Biosci. Eng.* **6** (2009), pp. 93–115.

[Pow75] Powell, C. et al. “Oral contraceptives and myocardial infarction in young women: a further report”. *BMJ* **3** (1975), pp. 631–632.

[Rei07] Reinecke, I. & Deuflhard, P. “A complex mathematical model of the human menstrual cycle”. *J. Theor. Biol.* **247** (2007), pp. 303–330.

[Rid97] Riddle, J. M. *Eve’s herbs: a history of contraception and abortion in the west*. Cambridge, Mass. : Harvard University Press, 1997.

[Rob13] Roblitz, S. et al. “A mathematical model of the human menstrual cycle for the administration of GnRH analogues”. *J. Theor. Biol.* **321** (2013), pp. 8–27.

[Rus94] Russell, J. C. et al. “Ever Since Eve: Birth Control in the Ancient World”. *Archaeology* **47** (1994), p. 29.

[Ryd67] Ryder, N. B. & Westoff, C. F. “United States: Methods of Fertility Control, 1955, 1960, & 1965”. *Stud. Fam. Plann.* **1** (1967), pp. 1–5.

[Sak93] Saketos, M. et al. “Suppression of the Hypothalamic-Pituitary-Ovarian Axis in Normal Women by Glucocorticoids”. *Biol. Reprod.* **49** (1993), pp. 1270–1276.

[Sch00] Schlosser, P. & Selgrade, J. “A model of gonadotropin regulation during the menstrual cycle in women: Qualitative features”. *Environ. Health Perspect.* (2000), pp. 873–881.

[ST05] Sciaky-Tamir, Y. et al. “Reproduction concepts and practices in ancient Egypt mirrored by modern medicine”. *Eur. J. Obstet. Gynecol.* **123** (2005), pp. 3–8.

[Sel10] Selgrade, J. “Bifurcation analysis of a model for hormonal regulation of the menstrual cycle”. *Math. Biosci.* **225** (2010), pp. 108–114.

[Sel99] Selgrade, J. & Schlosser, P. “A Model for the Production of Ovarian Hormones During the Menstrual Cycle”. *Fields Inst. Commun.* (1999), pp. 429–446.

[Sel09] Selgrade, J. et al. “A Model for Hormonal Control of the Menstrual Cycle: Structural Consistency but Sensitivity with Regard to Data”. *J. Theor. Biol.* **260** (2009), pp. 572–580.

[SW06] Sitruk-Ware, R. “New progestagens for contraceptive use”. *Hum. Reprod. Update* **12** (2006), pp. 169–178.

[Slo81] Slone, D. et al. “Risk of myocardial infarction in relation to current and discontinued use of oral contraceptives”. *NEJM* **305** (1981), pp. 420–424.

[Smi86] Smith, A et al. “Oral contraceptives and venous thromboembolism: findings in a large prospective study”. *BMJ* **292** (1986), p. 526.

[Sou93] Souza, M. D. et al. “High Frequency of Luteal Phase Deficiency and Anovulation in Recreational Women Runners: Blunted Elevation in Follicle-Stimulating Hormone Observed during Luteal-Follicular Transition”. *J. Clin. Endocr.* **83** (1993), pp. 4220–4232.

[Sta13] Stanczyk, F. Z. et al. “Ethinyl estradiol and 17β-estradiol in combined oral contraceptives: pharmacokinetics, pharmacodynamics and risk assessment”. *Contraception* **87** (2013), pp. 706–727.

[Tor97] Tornesi, M. “Estradiol up-regulates estrogen receptor and progesterone receptor gene expression in specific ovine uterine cells”. *Biol. Reprod.* **56** (1997), pp. 1205–1215.

[Tre67] Treloar, A. et al. “Variation of the human menstrual cycle through reproductive life”. *Int. J. Fertil.* **12** (1967), pp. 77–126.

[Tsa71] Tsai, C. & Yen, S. “The effects of ethinyl estradiol administration during early follicular phase of the cycle on the gonadotropin levels and ovarian function”. *J. Clin. Endocrinol.* **33** (1971), pp. 917–923.

[Ves70] Vessey, M. P. et al. “Thromboembolic Disease And The Steroidal Content Of Oral Contraceptives”. *BMJ* **2** (1970), pp. 203–209.

[Vin11] Vinther, F. et al. “The minimal model of the hypothalamic-pituitary-adrenal axis.” *Math. Biol.* **63** (2011), pp. 663–690.

[Wag05] Wagenmaker, E. et al. “Cortisol Interferes with the Estradiol-Induced Surge of Luteinizing Hormone in the Ewe”. *Biol. Reprod.* **80** (2005), pp. 458–463.

[Wan76] Wang, C. et al. “The functional changes of the pituitary gonadotrophs during the menstrual cycle”. *J. Clin. Endocrinol. Metab.* **42** (1976), pp. 718–728.

[Wel99] Welt, C. et al. “Female Reproductive Aging is Marked by Decreased Secretion of Dimeric Inhibin”. *J. Clin. Endocrinol. Metab.* (1999), pp. 105–111.

[Wen92] Wenk, R. et al. “How frequent is heteropaternal superfecundation?” *Acta Genet Med Gemellol (Roma)* **41** (1992), pp. 43–47.

[Wes97] Westergaard, T. et al. “Population based study of rates of multiple pregnancies in Denmark 1980-94”. *BMJ* **314** (1997), pp. 775–779.

[Wes76] Westoff, C. F. “The Decline of Unplanned Births in the United States”. *Science* **191** (1976), pp. 38–41.

[Wil88] Willett, W. C. et al. “A prospective study of moderate alcohol consumption and the risk of coronary disease and stroke in women”. *NEJM* **319** (1988), pp. 267–273.

[Yen05] Yen, S. et al. “The Human Menstrual Cycle: Neuroendocrine Regulation”. *Clin. Endocrinol.* **4** (2005), pp. 191–217.

[Yue06] Yue, H. et al. “Insights into the behaviour of systems biology models from dynamic sensitivity and identifability analysis: a case study of an NF-κB signalling pathway”. *Mol. Biosyst.* **2** (2006), pp. 640–649.

[Zel04] Zeleznik, A. “The physiology of follicle selection”. *Reprod. Biol. Endocrinol.* **2** (2004), p. 31.

[Zel94] Zeleznik, A. & Benyo, D. *The Physiology of Reproduction, Second Edition: Control of follicular development, corpus luteum function, and the recognition of pregnancy in higher primates*. Ed. by Knobil, E. & Neill, J. New York: Raven Press, Ltd., 1994.